

Growth of monazite during prograde metamorphism

Thesis submitted in accordance with the requirements of the University of Adelaide for an Honours Degree in Geology

Brendon John Liley

November 2014



THE UNIVERSITY
of ADELAIDE

GROWTH OF MONAZITE DURING PROGRADE METAMORPHISM

RUNNING TITLE: PROGRADE MONAZITE GROWTH

ABSTRACT

The reactions leading to monazite growth during progressive metamorphism are still not completely understood. This has a flow-on effect of not being able to completely and reliably link monazite U–Pb age data to specific parts of the P–T evolution of rocks. A suite of progressively contact-metamorphosed metapelites and metapsammities from Mt Stafford in central Australia were used to constrain metamorphic monazite growth mechanisms. U–Pb monazite geochronology is used to distinguish detrital (>1800 Ma) from metamorphic (<1800 Ma) monazite, and in granulite facies samples indicates that >50% of monazite is detrital. Differences in grain-separate yields are interpreted to reflect detrital and metamorphic monazite in greenschist facies samples being considerably finer-grained (<70 μm) than in granulite facies samples, since the sum of REE + Y + Th + U in samples is relatively uniform regardless of metamorphic grade. Comparatively low-Th rims on higher-Th monazite ‘cores’ in granulite facies samples are interpreted to reflect metamorphic monazite overgrowths on either detrital or (slightly) older metamorphic cores. Therefore, pre-existing monazite is interpreted as a major contributor to metamorphic monazite growth. Apatite—observed as inclusions in monazite—and xenotime, and possibly major silicate minerals such as plagioclase, biotite, muscovite and andalusite/sillimanite, are also interpreted to be contributors on the basis of their presence, their composition and, in the case of silicates, their vast abundance relative to monazite even if they only contain a minor amount of REEs. This study argues that pre-existing monazite is a major contributor to metamorphic monazite growth and therefore that the link between monazite growth and changes to P–T (as monitored by changes to silicate mineral assemblage) is not straightforward.

KEYWORDS

Metamorphism, Monazite, REEs, Mt Stafford, Metapelite, Psammite

TABLE OF CONTENTS

Growth of Monazite During Prograde Metamorphism	i
Running Title: Prograde monazite growth	i
Abstract.....	i
Keywords.....	i
List of Figures and Tables	2
Introduction	3
Background and Geological Setting.....	7
Methods	9
Sample Collection – Mt Stafford, Arunta Region NT.....	9
Sample Preparation – Whole-Rock Analysis	10
Sample Preparation – Thin Sections.....	10
Sample Preparation – Resin Mounts	10
Back-scattered Electron Imaging.....	11
Mineral Chemistry – Electron Probe Micro-analysis (Electron Microprobe)....	11
Geochronology – LA–ICP–MS	12
Observations and Results.....	12
Whole rock chemistry.....	12
Petrography.....	15
Monazite Composition and monazite element maps.....	17
Apatite and Xenotime Composition	23
Monazite U–Pb age data.....	23
Discussion	29
Chemical Characteristics of Detrital vs. Metamorphic Monazite	29
Why is monazite more abundant in high-grade samples?	31
Growth of monazite during progressive metamorphism	32
Conclusions	34
Acknowledgments	35
References	35
Appendix A: Whole-rock Geochemistry	38
Appendix B: Electron Microprobe Analyses.....	39
Appendix C: Monazite Geochronological Data	40

LIST OF FIGURES AND TABLES

Figure 1: Location map of Mt Stafford (Bottom) including zone boundaries indicating metamorphic grade (derived from Greenfield 1997), as well as a map of the wider Reynolds-Anmatjira Ranges (Taken from Morrissey et al. 2014).	6
Figure 2: A comparison of SiO_2 wt% concentration vs, Al_2O_3 wt% concentration in whole rock chemistry. The data is divided distinctly into two groups, with the SiO_2 rich group being designated psammitic, and the Al_2O_3 rich group being designated the pelitic.	13
Figure 3: Table of whole-rock compositions for samples in this study, oxides displayed in wt% and trace elements displayed in ppm. Sum total of REEs + Y + Th + U and calculated heat production for each sample is also displayed.	14
Figure 4: BSE images from sample STF 21c show cores of apatite with monazite overgrowth.....	20
Figure 5: BSE image and elemental maps of monazite grain from granulite facies sample STF 21a. Inclusions of apatite are clearly visible in Ca map (B), rim features are visible in Th map (D).	21
Figure 6: BSE image and elemental maps of monazite grain from granulite facies sample STF 21a. Internal grain complexity and rim features are apparent in each elemental map (B-E).....	22
Figure 7: Histograms of monazite ages for each metamorphic sample. Relative probability curves indicate the most probable mean age of monazite grains.....	24
Figure 8: Histograms of monazite ages for each igneous sample. Relative probability curves indicate the most probable mean age of monazite grains.	27
Figure 9: Concordia plots of each sample in this study.....	28
Figure 10: Comparison of wt% concentrations in element pairs; La vs. Ce, U vs Y and Th vs. Ca, in both pelitic samples and psammitic samples.....	29

INTRODUCTION

Monazite - $[\text{LREE,Y,Th,U,Ca}][\text{Si,P}]\text{O}_4$ - is a phosphate mineral that contains predominantly light rare-earth elements (LREE) as well as significant quantities of yttrium, thorium and uranium (Gebauer and Grünenfelder, 1979). Monazite occurs as an accessory mineral, primarily in aluminous metasedimentary and peraluminous igneous rocks. Monazite has been shown to grow as a metamorphic mineral during prograde (e.g. Smith and Barreiro 1999, Rubatto *et al.* 2001; Wing *et al.* 2003; Kohn & Malloy 2004; Corrie & Kohn 2008) and retrograde (Kelsey *et al.* 2003, 2007, 2008) metamorphism. Due to its typical exclusion of lead during formation, any lead that is found in monazite is interpreted as the radiogenic product of Th and U decay (Parrish 1990). Monazite is therefore one of the most commonly used minerals for determining the age of medium (~500 °C) to high (~1000 °C) temperature metamorphic processes.

In the past decade there has been and continues to be a significant effort to place monazite ages from metamorphic rocks in the context of the metamorphic pressure-temperature path. That is, to link geochronology with the physical and thermal processes of orogenesis and tectonics (e.g. Janots *et al.* 2007, 2008; Kelsey *et al.* 2008; Spear & Pyle 2010; Kali *et al.* 2010; Cubley *et al.* 2013; Korhonen *et al.* 2011; Warren *et al.* 2011; Anderson *et al.* 2013; Rubatto *et al.* 2013; Morrissey *et al.* 2014; Yakymchuk & Brown 2014) to better constrain rates and timescales. However, despite the widespread use of monazite for the purpose of U–Pb geochronology, there is little constraint on the pressure and temperature conditions at which monazite grows because the mineral reactions that are responsible for its formation remain largely unquantified (Janots *et al.* 2007; Kelsey *et al.* 2008; Pyle and Spear 2010; Spear 2010; Stepanov *et al.* 2012). Numerous studies have inferred mineralogical relationships between

monazite and various other minerals including allanite, apatite, xenotime, garnet, chlorite, biotite, andalusite, kyanite and staurolite that may contribute elements to monazite formation (Smith & Barreiro 1990; Pyle & Spear 1999; Wing *et al.* 2003; Kohn & Malloy 2004; Corrie & Kohn 2008; Janots *et al.* 2008). These studies have been largely qualitative or semi-quantitative at best, relying primarily on petrologic observations and interpretations, and exhibiting a paucity or lack of geochemical data on trace element changes within minerals and throughout mineral assemblages that were studied. Nevertheless, they have shed important light on our understanding of monazite growth during prograde metamorphism. However, due to the absence of systematic quantification of the solid solution composition of accessory and silicate minerals as a function of metamorphic grade, there is a gap in our knowledge resulting in an insufficient understanding of mineral reactions that cause monazite growth and destruction. Ultimately, this unresolved gap in knowledge hampers our efforts to reliably and robustly link metamorphic P - T paths with monazite ages with the timescales and rates of tectonic processes.

In order to address some of these deficiencies, this study aims to quantify assertions made by Wing *et al.* (2003), Kohn and Malloy (2004) and, Corrie and Kohn (2008), that major silicate as well as accessory minerals are involved in the prograde growth of monazite in metamorphic rocks. The approach taken to perform this quantification and propose reaction mechanisms by which monazite grows in metasedimentary rocks is specifically centred on conducting trace element analysis to quantify the abundance and distribution of trace elements in accessory minerals as a function of metamorphic grade and rock type. The ideal rock types for this project are metamorphosed shales and (impure) sands from a contact-metamorphosed setting because they allow sequential

progression of metamorphic grade to be studied and, due to their compact spatial distribution; they are also more likely to maintain compositional consistency across the entire range of metamorphic grades present. Other key criteria for rocks used in this study include a necessity that they are mineralogically responsive to changes in pressure and temperature, and that they encompass a wide range of metamorphic grades, in this case from low-grade (greenschist facies) to high-grade (granulite facies) metamorphic mineral assemblages. The sample suite used for this study is that from a well-documented contact-metamorphic setting, Mt Stafford, Arunta Region, Central Australia (Fig. 1). Rocks at Mt Stafford represent a rare example of an extremely well preserved metamorphic field gradient over a distance of approximately 10 km from greenschist through to granulite facies involving metamorphosed sands and shales (Greenfield et al. 1996, 1998; White et al 2003; Rubatto et al 2006). As such, the site represents an almost perfect natural laboratory in which a project of this kind can be undertaken.

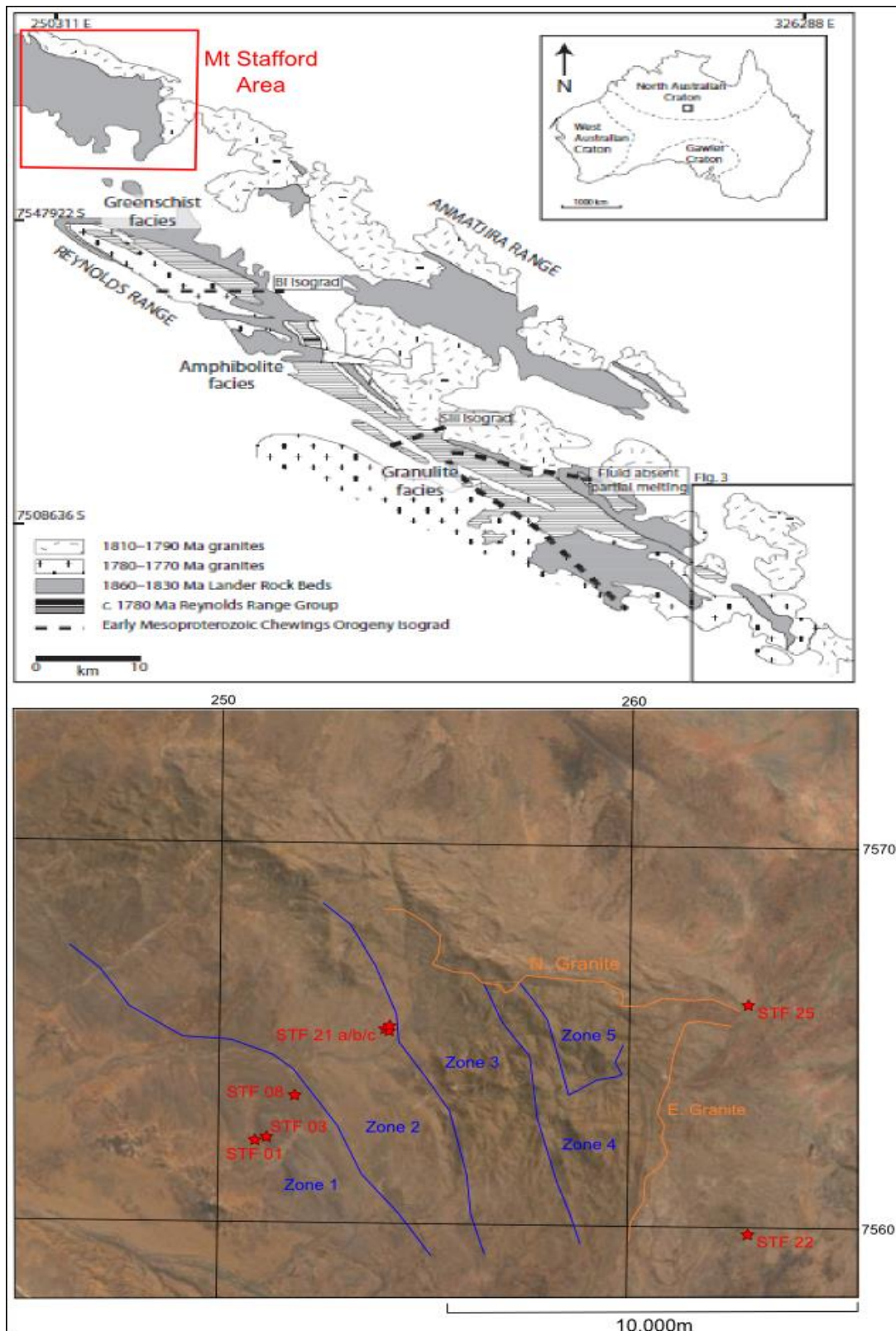
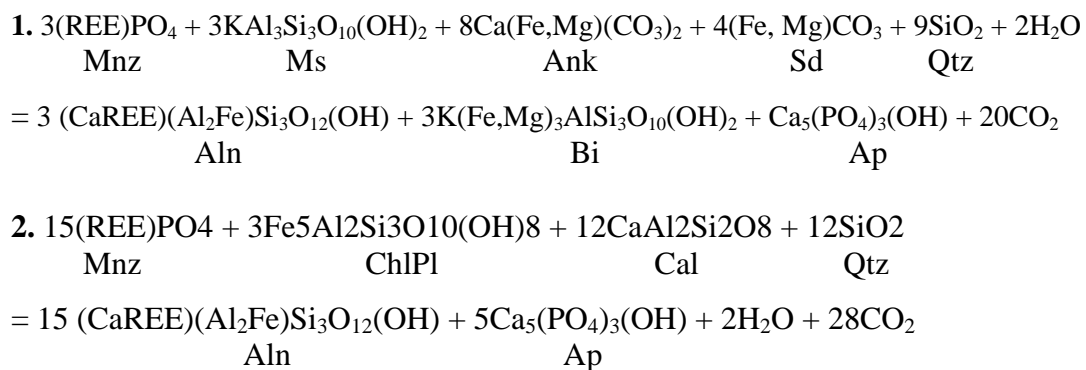
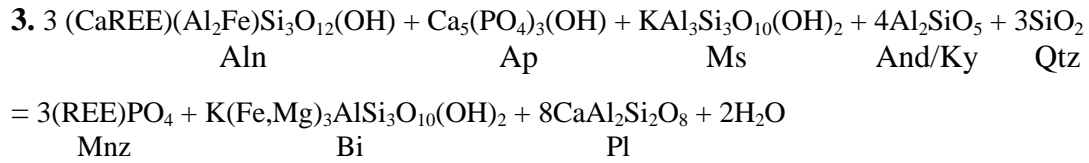


Figure 1: Location map of Mt Stafford (Bottom) including zone boundaries indicating metamorphic grade (derived from Greenfield 1997), as well as a map of the wider Reynolds-Anmatjira Ranges (Taken from Morrissey et al. 2014).

BACKGROUND AND GEOLOGICAL SETTING

Many studies have suggested possible connections between the growth and destruction of monazite with other phosphate or rare-earth element (REE) bearing minerals. It was suggested by Smith and Barreiro (1990) that allanite, another REE bearing mineral, might be a contributor of light REEs (or LREEs) to monazite growth due to its appearance in rocks upon the loss of monazite. Wing *et al.* (2003) substantiated this claim further with evidence presented that monazite disappears at the andalusite isograd, and the growth of new monazite occurs upon the disappearance of allanite at the andalusite/kyanite transition. Apatite and xenotime have similarly been suggested as contributors of Phosphorus (Janots *et al.* 2008; Bonyadi *et al.* 2011). Aluminosilicate minerals, andalusite and kyanite, as well as staurolite, an iron and aluminium bearing silicate mineral, have been inferred to be involved in monazite growth due to observations of monazite appearing or disappearing seemingly in correlation with the appearance or disappearance of these minerals (Kohn and Malloy 2004; Corrie and Kohn, 2008). Analyses of the relationship between garnet and various accessory phases in regard to the element yttrium have indicated that there is a strong chemical relationship between these minerals (Pyle and Spear, 1999). From all these studies, the mineral reactions that have been proposed to explain monazite growth include:





(Wing *et al.* 2003)

However, despite numerous studies making these and similar inferences, their claims have not been quantified in sufficient detail.

Mt Stafford is located at the NW end of the Anmatjira Ranges in the Palaeo- and Meso-Proterozoic Arunta Region, Northern Territory (Fig. 1). Mt Stafford provides an excellent exposure of progressively metamorphosed rocks that are derived from a common original rock unit (e.g. Greenfield *et al.* 1996; White *et al.* 2003).

The rocks of interest for this study are metamorphosed sedimentary rocks of the Mt Stafford beds that are considered to be part of the more regionally extensive Lander Formation (Claoué-Long *et al.*, 2008). The Mt Stafford beds were determined to have a maximum depositional age of c.1858 Ma (Claoué-Long *et al.*, 2008).

The Mt Stafford beds are composed of interbedded layers of originally sand-dominated (psammitic) and silt-dominated (pelitic) sediments, which are now metamorphosed.

The Mt Stafford beds were metamorphosed at shallow depths (very high thermal gradient conditions) at c. 1800-1830 Ma (Greenfield *et al.* 1996, 1998; Rubatto *et al.*, 2001), which resulted in the formation of a low pressure-high temperature contact aureole varying from greenschist to granulite facies toward the NE (Greenfield *et al.* 1996, 1998). The area is divided into five zones of progressively increasing metamorphic grade across a distance of just 10 km. (Fig. 1; Greenfield *et al.* 1996, 1998; White *et al.*, 2003)

Because the rocks of this area progress to higher metamorphic grade rapidly across a relatively short distance, the probability of sedimentary facies changes are likely reduced, and thus the site represents an almost perfect natural laboratory in which a project of this kind can be undertaken.

METHODS

A subset of samples was chosen from among those collected during fieldwork at Mt. Stafford upon which analyses were focussed. These samples were chosen to represent the low, medium and high grades of metamorphism in the study area (Fig. 1), and also to represent both a pelitic and a psammitic example within each grade. This selection was made in order to ensure that the analytical program contained chemical and isotopic data collected from rocks representative of the full range of metamorphic grade and rock type.

Sample Collection – Mt Stafford, Arunta Region NT

Five days of field sampling were undertaken at Mt. Stafford in April 2014. The primary objective of sampling was to collect a suite of pelitic and psammitic rocks from the progressive sequence of metamorphic grades. Samples of intrusive rocks from the north and eastern margins of Mt Stafford were also collected for the purpose of identifying emplacement ages and to thereby establish probable causation and timing of metamorphism. Samples were taken at sufficient size to ensure representative examples of outcrop were recovered. The samples were removed from outcrop using sledge and crack hammers as well as steel chisels at more resistive outcrops.

Sample Preparation – Whole-Rock Analysis

Whole-rock geochemical analysis was undertaken by Wavelength Dispersive x-ray Fluorescence (WD-XRF) spectrometry at the Earth and Environmental Department, Franklin and Marshall College, Lancaster PA, USA.

Major elements were analysed on fused discs prepared using a lithium tetraborate flux.

Iron content was determined by wet chemistry method.

Sample Preparation – Thin Sections

Large field samples were reduced to manageable size using a diamond-tungsten carbide rock-saw.

For in-house sections; once cut to appropriate sizes, rock blocks were adhered to glass slides using epoxy resin. The blocks were further cut down to thin slivers less than 5mm in thickness, then ground down to a thickness less than 0.5mm using coarse lapping discs. Polishing was undertaken using sandpaper with a fine grit, then finally with 1 μm diamond paste on a cloth lap to a thickness of 30 μm .

Additional polished thin sections were prepared by Continental Instruments, India.

Sample Preparation – Resin Mounts

Large field samples were reduced to manageable size using a diamond-tungsten carbide rock-saw.

Once reduced to suitable size, samples were crushed in a jaw-crusher, then subsequently milled to a fine grade in a ring mill. Sieving was undertaken to separate a coarseness fraction between 425 μm and 70 μm .

Crushed and sieved material was panned manually to concentrate dense mineral grains and to eliminate those of lower density. Magnetic separation was then undertaken using a Franz Isodynamic Separator to separate fractions <0.5 A, $0.5-0.8$ A and >0.8 A.

Density separation in a heavy liquid (Methylene Iodide) column was applied to the $0.5-0.8$ A fraction with the dense separate being preserved as that most likely to contain monazite.

Monazite fraction was mounted using epoxyure resin, then polished first using sandpaper with a fine grit, then with $1\mu\text{m}$ diamond paste on a cloth lap.

Back-scattered Electron Imaging

Thin sections and mounts were carbon coated prior to back-scattered electron (BSE) imaging. BSE Imaging of thin sections was done using a Philips XL30 FEGSEM with EDAX EDS at Adelaide Microscopy (University of Adelaide) to characterise and identify metamorphic mineral assemblages, to identify the microstructural location of monazite and other accessory mineral grains. Mosaics of BSE images were used to establish the abundance of monazite in each sample. Monazite was identified on account of its bright appearance in high contrast images, and then confirmed by use of EDAX. Images were produced with an accelerating voltage of 15kV , spot size of 5, and at a working distance of $10\ \mu\text{m}$.

Mineral Chemistry – Electron Probe Micro-analysis (Electron Microprobe)

Spot analyses of mineral compositions and elemental x-ray maps of monazite grains were obtained using a Cameca SXFive Electron Microprobe at Adelaide Microscopy (University of Adelaide). Rare-earth element concentrations in accessory minerals (e.g. monazite) were collected using a beam current of $100\ \text{nA}$ and an accelerating voltage of

15kV. Qualitative compositional maps of P, Ca, La, Ce, Y, Th, U and Pb in monazite and associated accessory phases were undertaken using a 15kV accelerating voltage and a beam current of 100 nA.

Geochronology - LA-ICP-MS

U–Pb geochronology of monazite was undertaken using a New Wave 213 nm Nd–YAG Laser paired with an Agilent 7500cx ICP–MS at Adelaide Microscopy (University of Adelaide). Analyses were done in a Helium atmosphere, with each spot consisting of 40 s of background measurement preceding 40 s of sample ablation. Prior to each ablation, 10 s is allowed for crystal and beam stabilisation. Beam size used was 20µm, frequency of 5hz and laser intensity of 100%. Data reduction was processed using the GLITTER software (Van Achterbergh *et al.* 2001, Griffin *et al.* 2008). Common lead was not corrected for in age calculations due to the unresolvable signal interference of ²⁰⁴Hg with the ²⁰⁴Pb isotope peak. The spectrometry for ²⁰⁴Pb was monitored for anomalous peaks as a proxy for common Pb, and those detected were eliminated age calculations.

OBSERVATIONS AND RESULTS

Whole rock chemistry

Tabulated whole rock compositional data for those samples used in this study are presented in Table 1, and data for all samples is presented in appendix A, and incorporates major and trace elements. A plot of SiO₂ wt% vs, Al₂O₃ wt% for all samples (Fig. 2), readily allows for distinction between metapelitic and metapsammitic samples, with metapelites having elevated Al₂O₃ wt% and reduced SiO₂ wt%. The sum total of REE + Y + Th+ U in each sample is relatively consistent across rock types and

with increasing metamorphic grade (Table 1; Appendix A). However, at the detail of specific elements, Ce for example, is distinctly higher in STF 01 than in other samples, whereas other elements, Th for example, shows less than 10 ppm variation across all primary samples.

Heat production calculated from whole-rock concentrations of K, Th and U at 1780 Ma (based on that being the most common metamorphic age peak in monazite age data, see monazite U-Pb age data) shows no obvious trend.

Of the 41 samples collected in the field, eight samples were selected for further analysis. Of these samples, two (2) are metapelite (a third metapelite, STF 07, of amphibolite-facies grade yielded no $>70\ \mu\text{m}$ monazite), four (4) are metapsammite, and two (2) are igneous (representing the eastern and northern granites). The results and discussion to follow are based only on these eight samples.

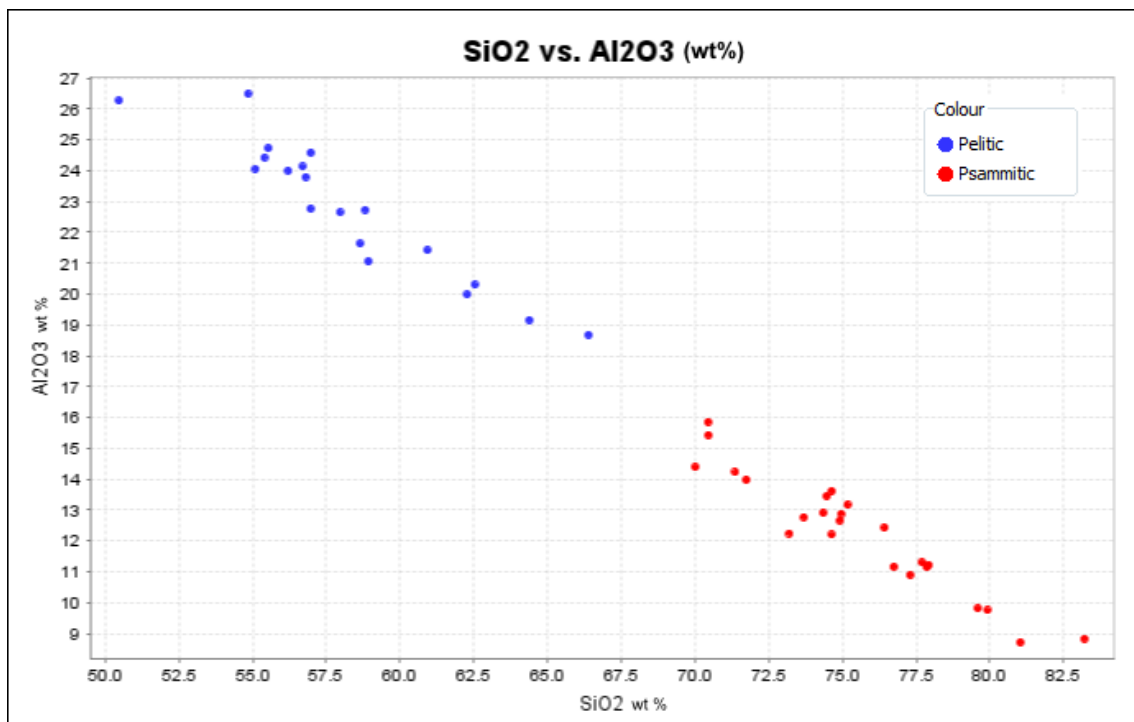


Figure 2: A comparison of SiO₂ wt% concentration vs, Al₂O₃ wt% concentration in whole rock chemistry. The data is divided distinctly into two groups, with the SiO₂ rich group being designated psammitic, and the Al₂O₃ rich group being designated the pelitic.

Specimen	STF 1	STF 3	STF-8	STF-21a	STF-21b	STF-21c	STF-22	STF-25
SiO ²	56.95	74.91	77.94	74.95	76.43	58.82	74.64	77.86
TiO ²	0.58	0.46	0.39	0.51	0.43	0.71	0.31	0.25
Al ² O ³	22.77	12.67	11.23	12.89	12.43	22.74	13.62	11.15
Fe ² O ³ T	9.00	4.35	3.79	4.28	4.22	6.79	2.49	2.18
MnO	0.11	0.06	0.11	0.06	0.05	0.09	0.05	0.04
MgO	2.72	1.25	1.05	1.19	1.19	2.07	0.71	0.30
CaO	0.48	0.63	0.78	1.00	0.39	0.33	1.15	0.86
Na ² O	0.40	0.86	0.72	1.08	0.75	1.22	1.94	1.77
K ² O	5.98	3.84	3.12	2.98	3.20	6.23	4.23	4.74
P ² O ⁵	0.14	0.11	0.10	0.11	0.11	0.12	0.13	0.11
LOI	1.74	0.71	0.85	0.50	0.52	0.60	0.81	0.79
Total	100.87	99.85	100.08	99.55	99.72	99.72	100.08	100.05
Rb	342.1	235.3	172.2	159.9	154.3	343.0	258.9	550.3
Sr	28	35	192	67	42	75	102	42
Y	23.4	23.1	20.1	20.4	20.0	24.1	9.5	60.1
Zr	85	200	245	234	213	128	196	248
V	76	47	44	45	39	72	30	17
Ni	46	28	25	26	27	46	16	9
Cr	52	38	48	50	34	68	32	11
Nb	17.6	14.5	12.0	15.2	11.4	19.2	10.8	12.6
Ga	32.2	19.9	16.9	19.2	18.6	33.5	20.8	17.9
Cu	38	12	14	6	12	10	12	11
Zn	144	65	63	64	63	111	37	33
Co	27	11	7	9	8	17	1	<1
Ba	804	535	719	504	521	798	462	201
La	41	39	37	39	34	37	29	36
Ce	106	70	87	64	69	78	56	71
U	<0.5	1.8	0.9	1.3	2.6	1.6	<0.5	1.8
Th	39.0	34.0	31.0	29.1	36.6	31.8	25.3	65.1
Sc	15	7	4	8	6	11	3	3
Pb	11	9	15	18	8	19	17	21
Sum total: REE, Y, Th and U	209.9	167.9	176	154.7	162.2	172.5	120.3	234
Heat Production (μW/m ³)	4.35	3.99	3.31	3.27	4.34	4.22	2.95	6.57

Figure 3: Table of whole-rock compositions for samples in this study, oxides displayed in wt% and trace elements displayed in ppm. Sum total of REEs + Y + Th + U and calculated heat production in μW/m³ for each sample is also displayed.

Petrography

STF 01 – Metapelite, Greenschist facies

Biotite and chlorite are abundant and muscovite is present in small quantities. These minerals have coarseness of (~25 μm), and do not show alignment to any obvious fabric. Quartz and poikiloblastic cordierite (~100 μm) are common, and comprise a large fraction of the mineralogy. Some coarse andalusite is present (~100 μm), which shows embayment at grain margins and minor skeletal growth features. Distinct pleochroic radiation-damage halos are present in biotite, although few of these are cored by minerals of sufficient size to be resolvable at the available magnification.

STF 03 - Metapsammite, Greenschist facies

Biotite and chlorite are abundant and muscovite is present in small quantities. These minerals have coarseness of (~25 μm), and do not show alignment to any obvious fabric. Biotite possesses distinct pleochroic radiation-damage halos. Quartz and plagioclase are common as well as some poikiloblastic andalusite. Coarse poikiloblastic cordierite (300 μm) is present.

STF 08 – Metapsammite, Amphibolite facies

Coarse grained quartz is dominant (100-700 μm), with significant interstitial platy biotite and minor chlorite. Opaque Fe-Ti oxide minerals are common, existing as inclusions within quartz, but more often at grain boundaries of major minerals. Skeletal/poikiloblastic andalusite is found in aggregates associated with micaceous minerals, especially biotite. Distinct pleochroic radiation-damage halos are present in low abundance in biotite grains.

STF 21a – Metapsammite, Granulite facies

Very coarse quartz and k-feldspar (200-500 μm) are dominant. Coarse platy biotite (100-300 μm) is common, and shows no alignment to fabric. Opaque Fe-Ti oxide minerals between (20-200 μm) are common, occurring as inclusions and at grain boundaries, with coarser grains appearing largely at grain boundaries rather than as inclusions. Skeletal aggregates of andalusite are seen commonly in association with biotite. Large pleochroic radiation-damage halos are rarely present in biotite grains, some with visible (10 μm) grains of monazite at their centres.

STF 21b – Metapsammite, Granulite facies

Coarse quartz and k-feldspar (200-500 μm) are dominant, with abundant interstitial aggregates of coarse skeletal andalusite. Coarse platy biotite grains (100 μm) are present, but not common. Finer grained biotite is seen in association with andalusite. Pleochroic radiation-damage halos are commonly present in biotite, most commonly in biotite that is in contact with andalusite. Coarse opaque Fe-Ti oxide minerals are common at grain boundaries, and some small opaque grains occur as inclusions in quartz.

STF 21c – Metapelite, Granulite facies

Very coarse quartz and k-feldspar (200-1000 μm) are abundant and contain many small inclusions of biotite. Interstitial aggregates of coarse skeletal andalusite are associated with fine to coarse (100-600 μm) grains of biotite. Large pleochroic radiation-damage

halos are common in biotite grains. Coarse (100-150 μm) opaque minerals are rarely present at grain boundaries, with occasional grains seen at (200-250 μm) in size.

STF 22 – Eastern Granite

Very coarse (1 mm) quartz and plagioclase comprise the majority of the sample, with plagioclase exhibiting distinctive twinning features. Biotite and muscovite commonly form aggregates throughout. Anhedral and amorphous opaque Fe-Ti oxide minerals are occasionally seen at grain boundaries.

STF 25 – Northern Granite

This very coarse-grained granite displays abundant rapakivi textures at outcrop scale. Coarse to medium grained quartz and plagioclase (200-400 μm) are dominant, with occasional extremely coarse, potentially porphyritic plagioclase grains (>2-3 mm). Coarse platy muscovite (~100-300 μm) is present, but not abundant. Anhedral biotite grains (~100 μm) are seen occasionally. Few anhedral and amorphous opaque Fe-Ti oxide grains are seen, although these are rare.

Monazite Composition and monazite element maps

EPMA spots were analysed on eight samples, with a total of 495 analyses being recorded, to characterise the solid-solution composition of monazite as a function of rock-type and metamorphic grade. Elements that were analysed were; Si, P, La, Ce, Ca, O, Zr, Pb, Th, U, Y, Pr, Nd, Sm and Gd. The full dataset is located in appendix B. Low monazite yields (<50 grains) of size >70 μm were obtained by heavy liquid separation for samples STF 01, 03 and 08. High yields (approximately >300 grains) were obtained >70 μm in samples STF 21a,b and c.

STF 01 – Pelite, Greenschist facies

Monazite in this sample exhibits values for La ranging from 9.05 to 13.54 wt%, Ce ranging from 20.95 to 25.89 wt%, Y ranging from 1.39 to 3.59 wt%, Th ranging from 0.05 to 12.69 wt %, U ranging from 0.08 to 0.72 wt%, and Ca ranging from 0.19 to 1.59 wt%. ($n=17$)

STF 03 – Psammite, Greenschist facies

Monazite in this sample exhibits values for La ranging from 9.87 to 14.13 wt%, Ce ranging from 20.26 to 26.93 wt%, Y ranging from 0.01 to 1.55 wt%, Th ranging from 2.11 to 12.17 wt %, U ranging from 0.02 to 0.39 wt%, and Ca ranging from 0.08 to 1.85 wt%. ($n=18$)

STF 08 – Psammite, Amphibolite facies

Monazite in this sample exhibits values for La ranging from 7.15 to 13.25 wt%, Ce ranging from 15.50 to 24.66 wt%, Y ranging from 1.18 to 3.33 wt%, Th ranging from 3.19 to 20.08 wt %, U ranging from 0.10 to 0.71 wt%, and Ca ranging from 0.49 to 3.30 wt%. Monazites in this sample show a relatively even spread of Th concentrations, rather than including any anomalously high outlying data points. ($n=25$)

STF 21a – Psammite, Granulite facies

Monazite in this sample exhibits values for La ranging from 8.36 to 12.96 wt%, Ce ranging from 19.96 to 25.99 wt%, Y ranging from 0.14 to 4.17 wt%, Th ranging from

3.01 to 11.54 wt %, U ranging from 0.05 to 01.54 wt%, and Ca ranging from 0.18 to 1.55 wt%. ($n=102$)

STF 21b – Psammite, Granulite facies

Monazite in this sample exhibits values for La ranging from 7.49 to 13.01 wt%, Ce ranging from 20.33 to 26.37 wt%, Y ranging from 0.35 to 3.18 wt%, Th ranging from 2.63 to 13.29 wt %, U ranging from 0.03 to 1.87 wt%, and Ca ranging from 0.13 to 1.76 wt%. ($n=85$)

STF 21c – Pelite, Granulite facies

Monazite in this sample exhibits values for La ranging from 10.45 to 12.82 wt%, Ce ranging from 21.50 to 24.84 wt%, Y ranging from 1.65 to 3.97 wt%, Th ranging from 2.92 to 6.06 wt %, U ranging from 0.15 to 0.80 wt%, and Ca ranging from 0.63 to 1.15 wt%. ($n=110$)

STF 22 – Eastern Granite

Monazite in this sample exhibits values for La ranging from 8.65 to 11.21 wt%, Ce ranging from 19.73to 23.87 wt%, Y ranging from 1.23 to 3.53 wt%, Th ranging from 5.33 to 7.92 wt %, U ranging from 0.25 to 1.31 wt%, and Ca ranging from 0.87 to 1.33 wt%. ($n=70$)

STF 25 – Northern Granite

Monazite in this sample exhibits values for La ranging from 6.44 to 10.98 wt%, Ce ranging from 17.52 to 25.12 wt%, Y ranging from 1.13 to 4.83 wt%, Th ranging from

6.08 to 14.83 wt %, U ranging from 0.01 to 0.41 wt%, and Ca ranging from 0.26 to 2.17 wt%. ($n= 60$)

BSE images of monazite from sample 21c show monazite grains cored by apatite (Fig. 4). Additionally, elemental maps of monazite grains reveal highly complex internal zoning in several grains (Fig. 5 and 6). Some monazite grains show a distinct rim of lower Th around a higher Th core(s) (Fig. 5 and 6) Inclusions of apatite were identified in several monazite grains in sample 21a (Fig. 5).

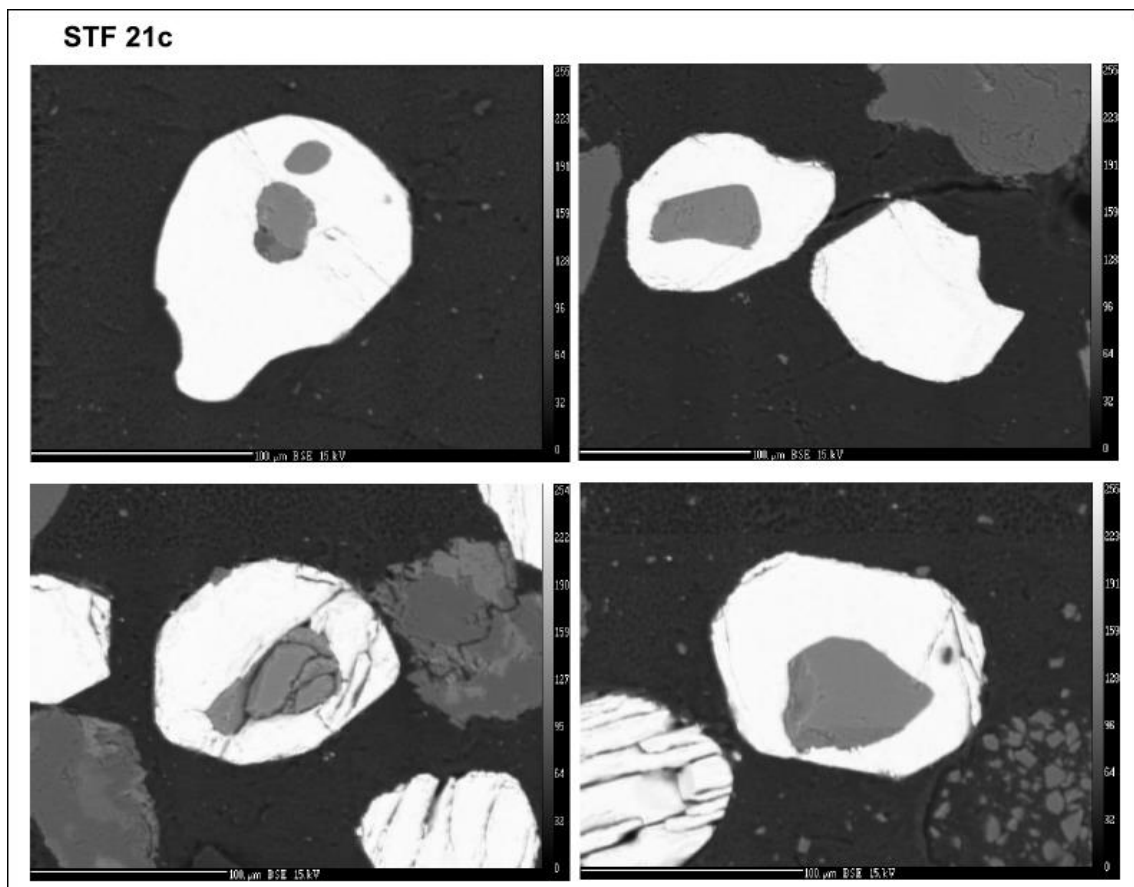


Figure 4: BSE images from sample STF 21c show cores of apatite with monazite overgrowth.

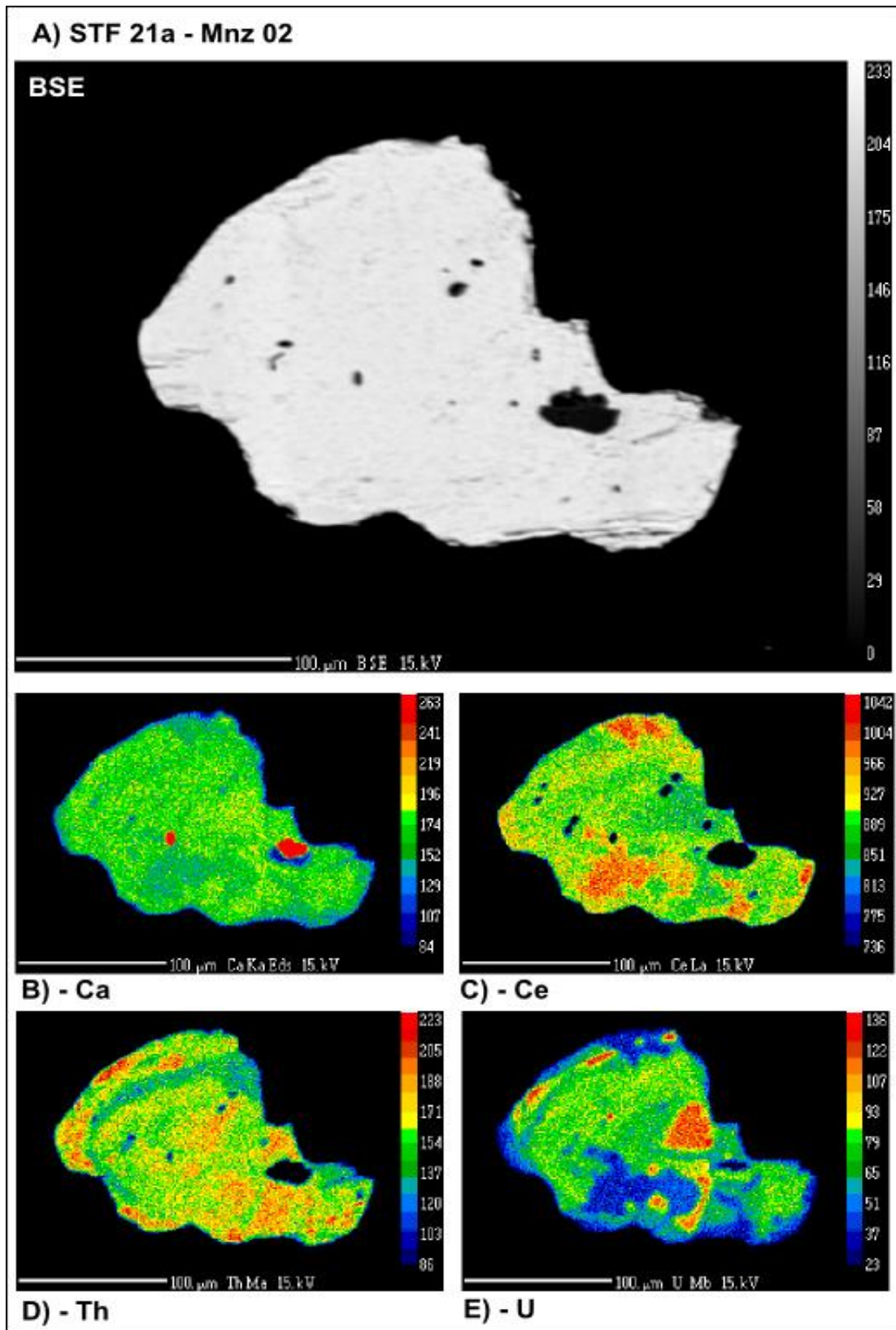


Figure 5: BSE image and elemental maps of monazite grain from granulite facies sample STF 21a. Inclusions of apatite are clearly visible in Ca map (B), rim features are visible in Th map (D).

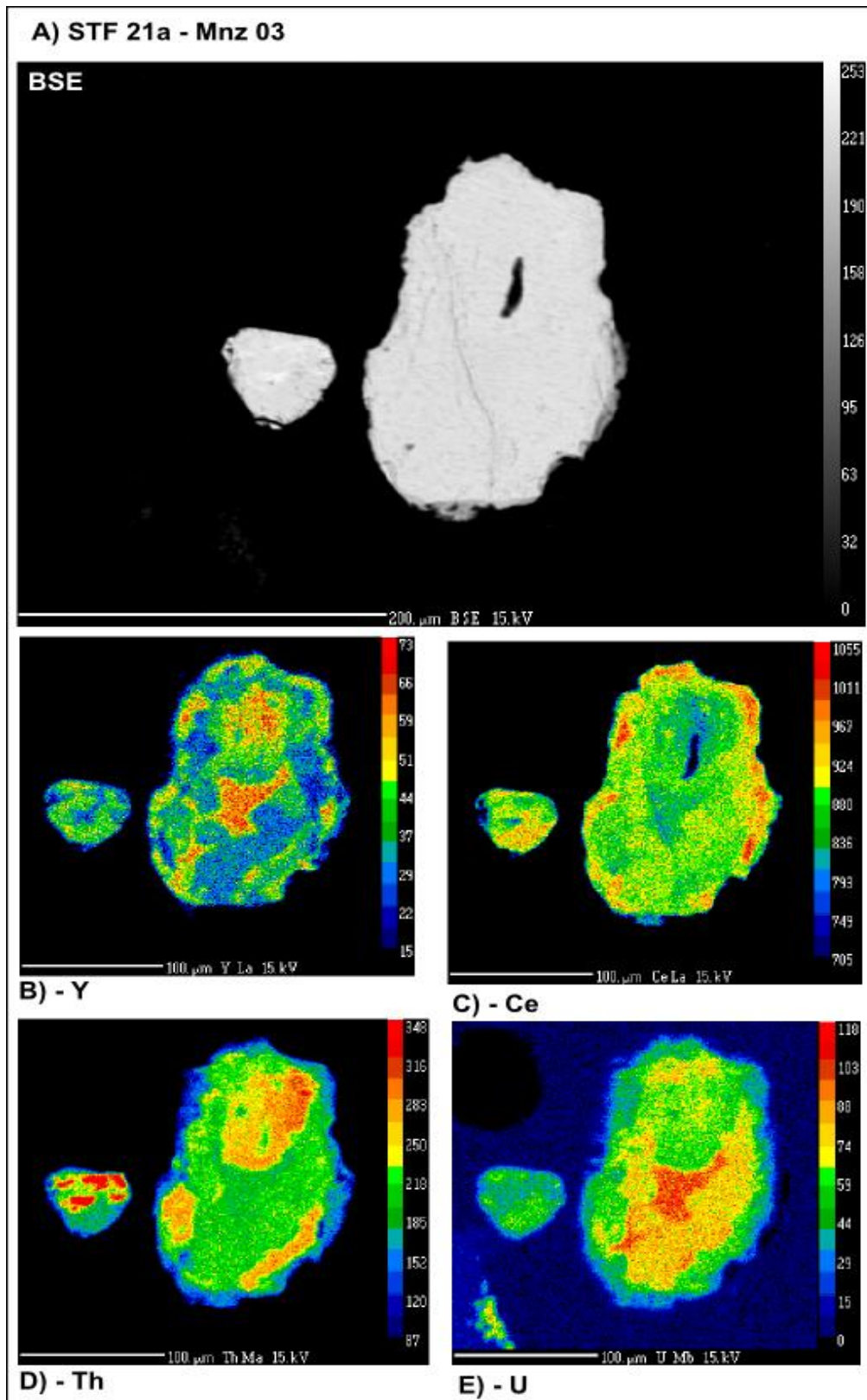


Figure 6: BSE image and elemental maps of monazite grain from granulite facies sample STF 21a. Internal grain complexity and rim features are apparent in each elemental map (B-E)

Apatite and Xenotime Composition

Apatite and xenotime were only found in sample STF 21c, where four apatite cores were found with monazite overgrowth and a single grain of xenotime was analysed. In this sample, apatite exhibits values for P ranging from 19.15 to 19.57 wt%, La ranging from 0.08 to 0.27 wt%, Ce ranging from 0.11 to 0.5 wt%, Y ranging from 0.15 to 0.33 wt%, Th ranging from 0.0 to 0.09 wt %, U ranging from 0.0 to 0.002 wt%, and Ca ranging from 37.16 to 37.86 wt%. ($n=4$)

Xenotime exhibits a value for P of 14.93 wt%, La of 0.13 wt%, Ce of 0.18 wt%, Y of 42.76 wt%, Th of 0.56 wt %, U of 0.66 wt%, and Ca of 0.18 wt%. ($n=1$)

Monazite U–Pb age data

Diagrammatic representation of LA–ICP–MS U–Pb age data for monazite is presented in Fig. 7 and 8, and analytical data are presented in appendix C. Monazite U-Pb age data was collected for the purpose of distinguishing metamorphic monazite grown during the Stafford Event (Greenfield *et al.* 1996, 1998; Rubatto *et al.*, 2001), from older detrital monazite.

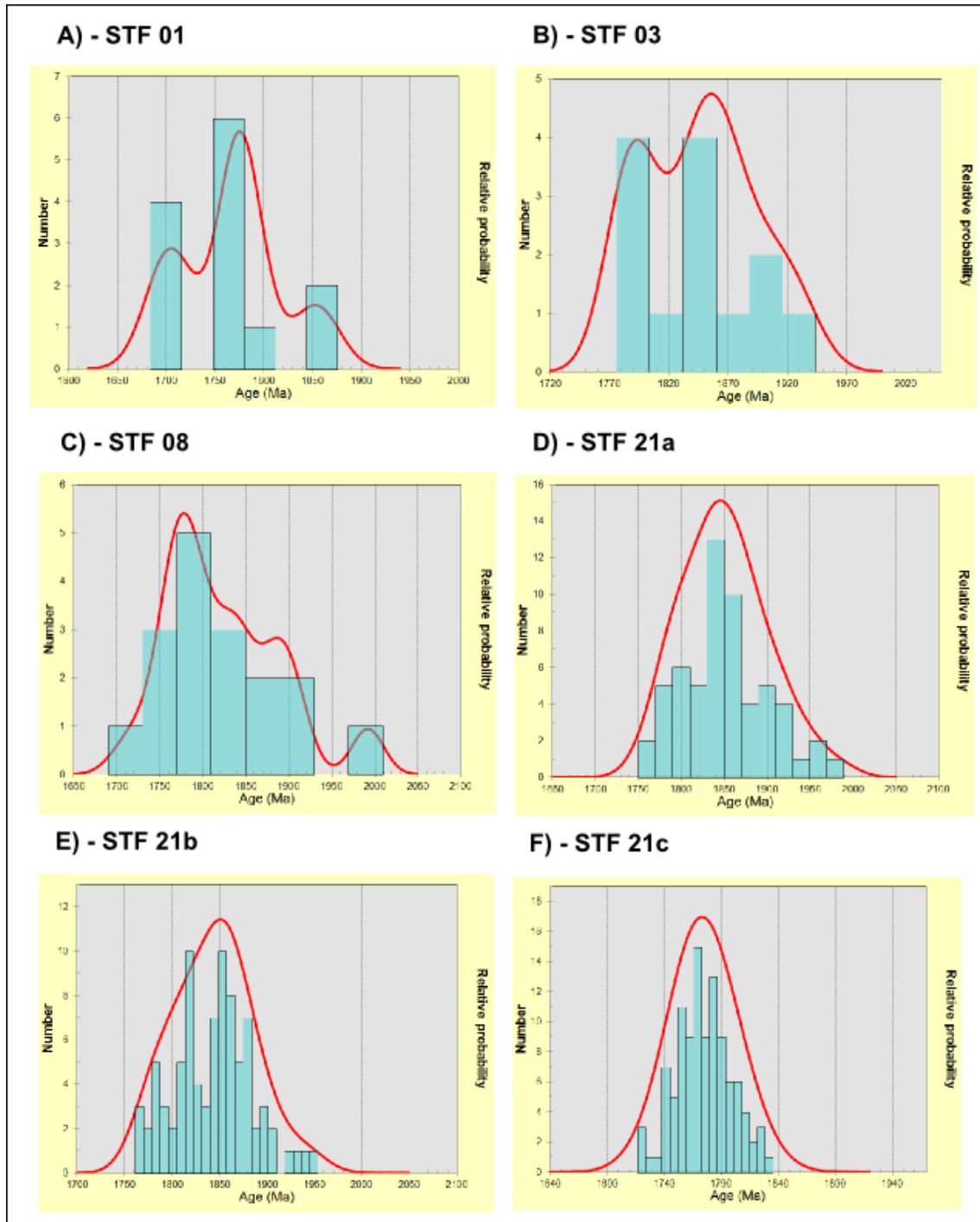


Figure 7: Histograms of monazite ages for each metamorphic sample. Relative probability curves indicate the most probable mean age of monazite grains.

STF 01 – Metapelite, Greenschist facies

Seventeen analyses were conducted on sample STF 01, four of which were excluded from final age estimates due to appreciable amounts of common lead (^{204}Pb). A probability density histogram was produced using $^{206}\text{Pb}/^{207}\text{Pb}$ ages, which presented a peak probability age of 1775 Ma (Fig. 7, A).

STF 03 – Metapsammite, Greenschist facies

Fifteen analyses were conducted on sample STF 03, two of which were excluded from final age estimates due to appreciable amounts of common lead (^{204}Pb). A metamorphic age for this sample could not be calculated as the younger ages are discordant (Fig. 9, A) However, a probability density histogram was produced using $^{206}\text{Pb}/^{207}\text{Pb}$ ages, which shows two peak probability ages of 1793.2 Ma and 1855.6 Ma (Fig. 7, B).

STF 08 – Metapsammite, Amphibolite facies

Eighteen analyses were conducted on sample STF 08, one of which was excluded from final age estimates due to appreciable amounts of common lead (^{204}Pb). A concordia age of 1804 ± 7.1 Ma (n=4) is estimated as the metamorphic age in this sample but is only on the basis of 4 concordant analyses as all the other analyses are older or slightly discordant (Fig. 9, B). A probability density histogram was produced using $^{206}\text{Pb}/^{207}\text{Pb}$ ages, which presented three peak probability ages of 1776.8 Ma, 1886.2 Ma and 1991.2 Ma (Fig 7. C).

STF 21a – Metapsammite, Granulite facies

Sixty analyses were conducted on sample STF 21a, two of which were excluded from final age estimates due to appreciable amounts of common lead (^{204}Pb). A concordia age of 1801.7 ± 9.2 Ma (n=19) is estimated as the metamorphic age in this sample (Fig. 9, C). A probability density histogram was produced using $^{206}\text{Pb}/^{207}\text{Pb}$ ages, which presented a peak probability age of 1850 Ma (Fig 7. D).

STF 21b – Metapsammite, Granulite facies

Eighty-five analyses were conducted on sample STF 21b. A concordia age could not be calculated for this sample. However, thirty-two analyses plotted on concordia indicate an age of c. 1800 Ma (n=32) (Fig. 9, D). A probability density histogram was produced using $^{206}\text{Pb}/^{207}\text{Pb}$ ages, which presented a peak probability age of 1846.12 Ma (Fig 7. E).

STF 21c – Metapelite, Granulite facies

One-hundred and ten analyses were conducted on sample STF 21c, four of which were excluded from final age estimates due to appreciable amounts of common lead (^{204}Pb). A concordia age of 1774.4 ± 1.9 Ma (n=92) is estimated for this sample (Fig. 9, E). A probability density histogram was produced using $^{206}\text{Pb}/^{207}\text{Pb}$ ages, which presented a peak probability age of 1769 Ma (Fig 7. F).

STF 22 – Eastern Granite

Seventy analyses were conducted on sample STF 22, three of which were excluded from final age estimates due to appreciable amounts of common lead (^{204}Pb). An age of

c. 1775 Ma is estimated based on the concordia age (Fig. 9, F). A probability density histogram was produced using $^{206}\text{Pb}/^{207}\text{Pb}$ ages, which presented a peak probability age of 1780 Ma (Fig 8. A).

STF 25 – Northern Granite

Sixty analyses were conducted on sample STF 25, seventeen of which were excluded from final age estimates due to appreciable amounts of common lead (^{204}Pb). The data define a spread on concordia, with concordant analyses occurring at c. 1610 Ma, c. 1700 Ma and c. 1770 Ma (Fig. 9, G). A probability density histogram was produced using $^{206}\text{Pb}/^{207}\text{Pb}$ ages, which presented three peak probability ages of 1616.8 Ma, 1760 Ma and 1914 Ma (Fig 8. B).

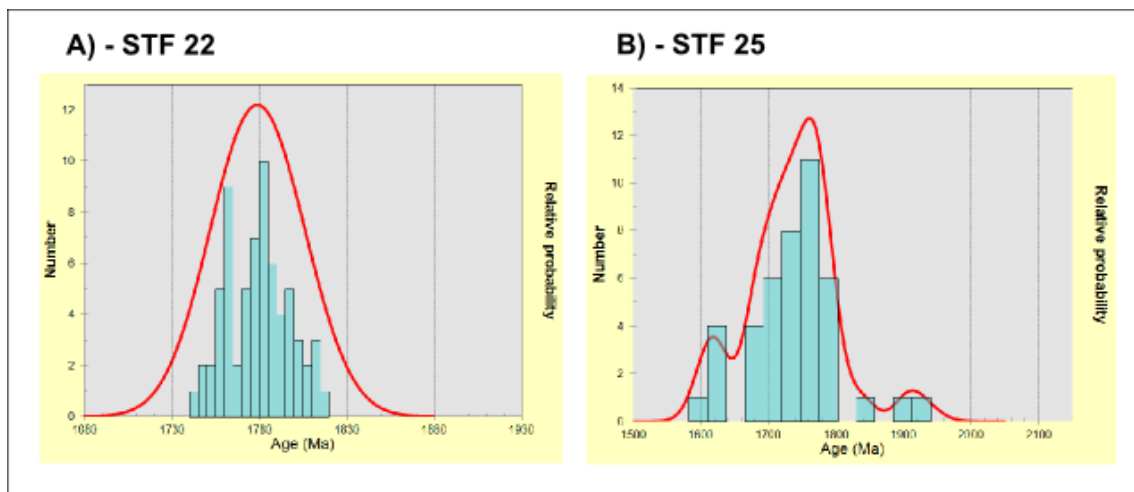


Figure 8: Histograms of monazite ages for each igneous sample. Relative probability curves indicate the most probable mean age of monazite grains.

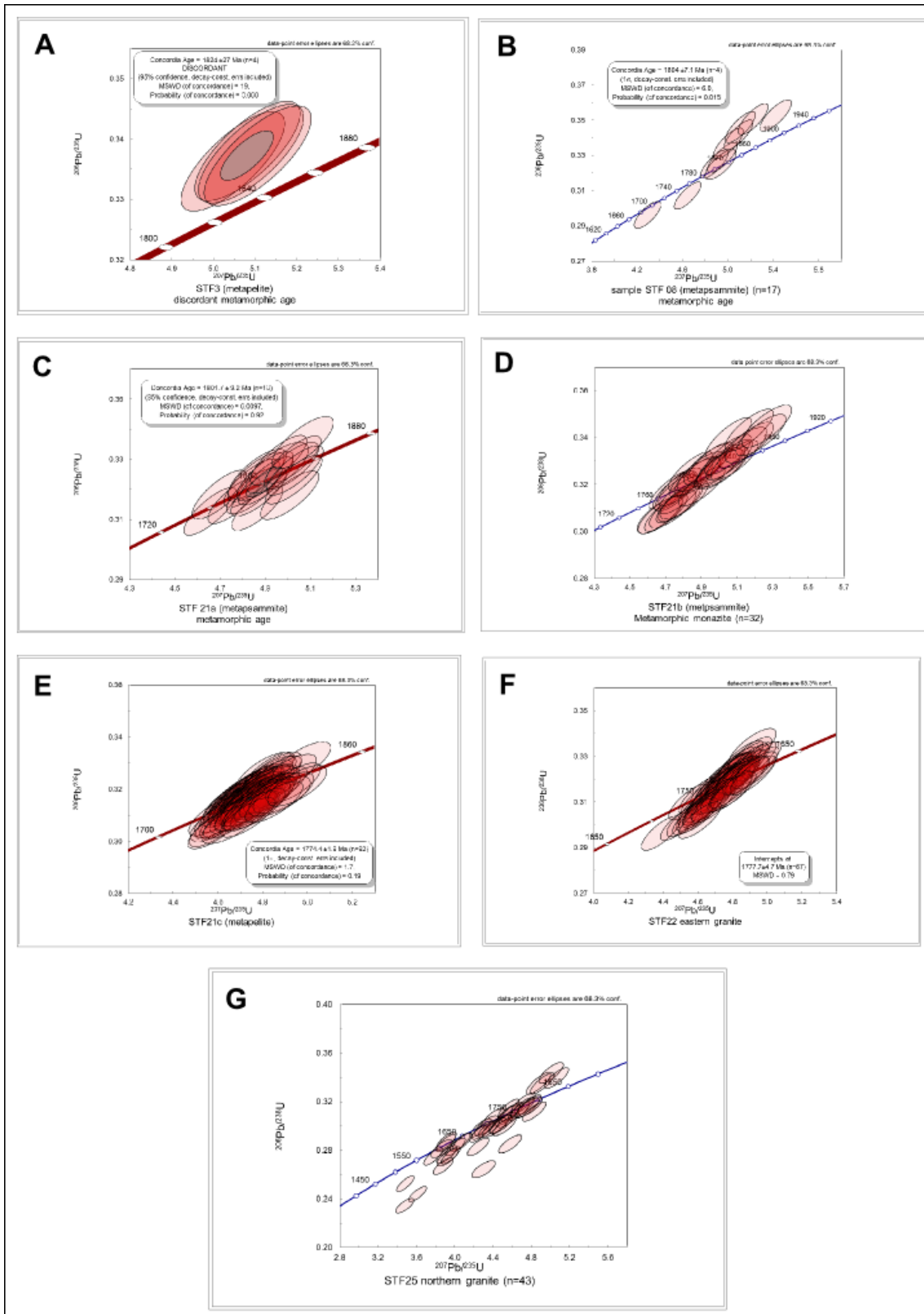


Figure 9: Concordia plots of each sample in this study.

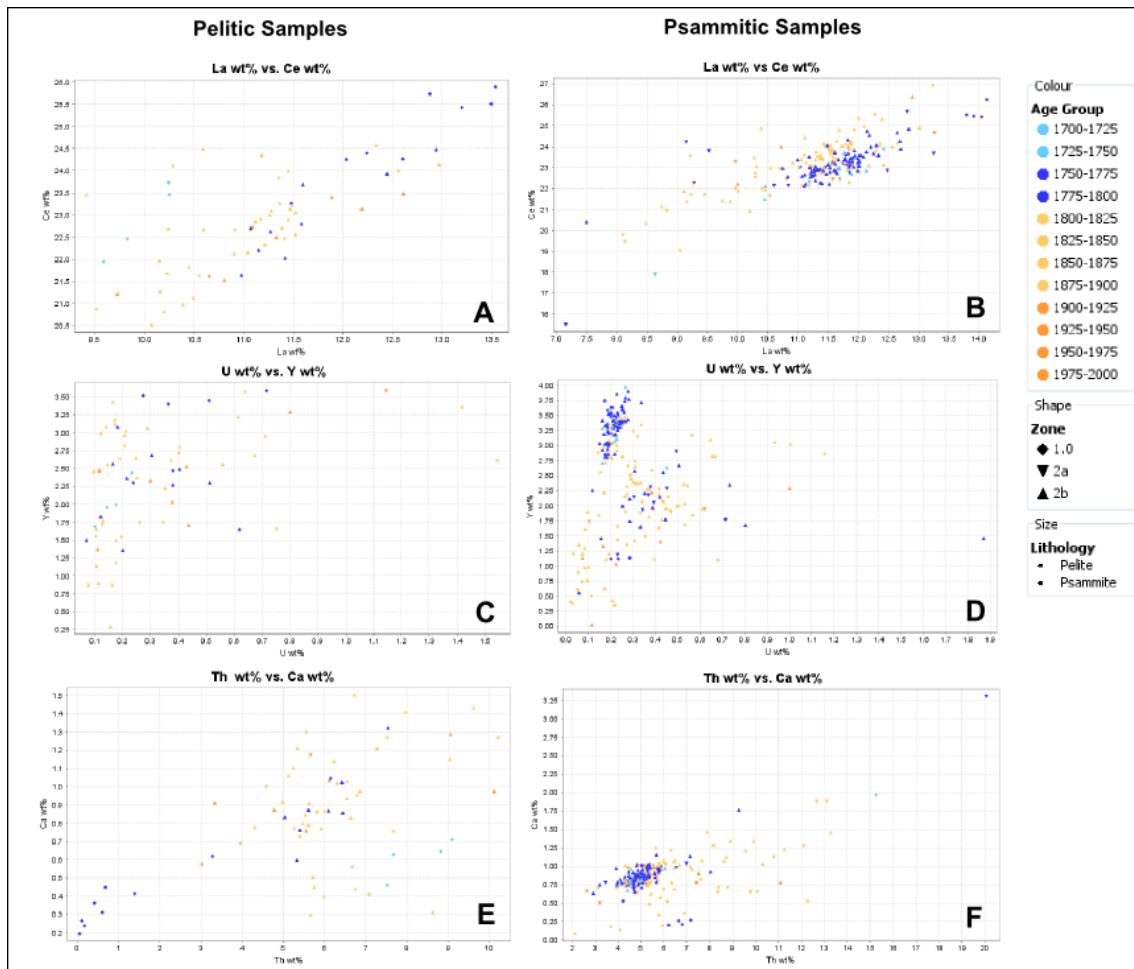


Figure 10: Comparison of wt% concentrations in element pairs; La vs. Ce, U vs Y and Th vs. Ca, in both pelitic samples and psammitic samples.

DISCUSSION

Chemical Characteristics of Detrital vs. Metamorphic Monazite

U-Pb geochronology was obtained for each monazite grain that was analysed for elemental composition using the electron microprobe. Using these datasets together, it is possible to classify grains into age groups that correspond to those grains that formed prior to the deposition of the Mt Stafford beds, which are therefore detrital, and those that formed subsequent to deposition, which therefore must be the result of the metamorphism that these rocks have experienced. The maximum depositional age constraint of c. 1858 Ma for the Mt Stafford beds is based on a study of detrital zircons

(Claoué-Long et al 2008). Therefore, using this constraint on depositional age, the threshold age for metamorphic grains is set here at 1800 Ma. Monazite compositional and age data was plotted comparing numerous elements to detect chemical differences between detrital and metamorphic grains in both pelitic samples and psammitic samples (Fig. 10). The elements used for plots shown here, Fig. 10, to identify differences between detrital and metamorphic monazite were chosen on the basis that of all analysed REEs, these are the ones that showed differences between age groupings in either metapelitic or metapsammitic rocks, or both.

Comparison of La vs. Ce for monazite in pelitic samples (Fig. 10, A) shows no particular trends, with data points from both metamorphic and detrital groups appearing to be scattered. The same comparison in psammitic samples (Fig. 10, B) reveals a relatively tight distribution of composition among metamorphic grains, whereas detrital grains show greater compositional variation. This may reflect a single reaction process being responsible for metamorphic grain growth vs. multiple sources for detrital grains. Comparison of U vs. Y (Fig. 10, C and D) shows similar results to that above, with monazite in pelitic samples exhibiting compositional scatter, and monazite in psammitic samples exhibiting a distinct compositional cluster among most metamorphic monazite grains and compositionally diverse detrital grains.

A final comparison of Th vs. Ca (Fig. 10, E and F) again exhibits similar features.

Monazite in pelitic samples shows significant compositional spread, whereas monazite in psammitic samples shows a tighter compositional cluster for metamorphic grains.

At least for psammitic samples, it seems reasonable that metamorphic monazite has been largely or wholly derived from a single metamorphic event, the P - T conditions of which have driven the formation of monazite of a particular composition. However, this

is not to say that all metamorphic monazite necessarily grew at the same P - T conditions (cf. Kelsey et al. 2008). On the other hand, metamorphic monazite in pelitic samples does not show obvious chemical similarity, perhaps due to additional mineral reaction processes being viable in metapelitic rocks as P - T increases, or perhaps due in part to being represented by fewer monazite grains in this study.

Why is monazite more abundant in high-grade samples?

High-grade samples STF 21a, b, c, provided a significantly greater yield of monazite grains upon separation using heavy liquids than low and medium-grade samples.

However, whole rock data shows that across all samples there is no major variation in the sum total of elements that form monazite (See Table 1) suggesting that there should be similar abundances of monazite in all samples, regardless of metamorphic grade.

The first possibility to consider is that monazite grains in low and medium-grade samples are similarly abundant in these rocks as they are in high-grade samples, but that grains are sufficiently small that they were not captured in the 425 μ m–70 μ m fraction during sieving. If this is the case, monazite grains in high-grade samples are coarser grained than those in lower-grade samples, consistent with grain coarsening that typically occurs with increasing metamorphic grade (e.g. Powell 1987) That is, if small grains are recrystallising and/or increasing in size as a result of prograde metamorphism, a larger number of them would become coarse enough to be captured at >70 μ m. Element maps of large monazite grains from sample 21c show distinct internal complexity including possible rims of metamorphic overgrowth (fig. 3 and 4). These maps of monazite could show evidence that originally detrital grains have served as nuclei for metamorphic monazite to grow on during progressive metamorphism.

A second mechanism by which monazite grains in the size range 425–70 μ m could become more abundant with grade, is that of melt-loss from high-grade samples. (e.g. Brown 1994). If minerals other than monazite are breaking down and their elements are partitioning into melt, it follows that the total volume of non-monazite minerals diminishes with loss of melt. It has been shown, that there is no requirement that all monazite dissolve into melt by the peak of metamorphism (Kelsey *et al.* 2008; Yakymchuk and Brown 2014), and therefore monazite could potentially become concentrated in the residual granulite facies rock. However, melt loss is not interpreted to have a significant effect on concentrating monazite in the high-grade samples studied here, since the sum total of REE + Y + Th + U (Table 1) in all samples is relatively uniform regardless of metamorphic grade.

A third option, the greater yield of monazite from the high-grade samples may reflect that actual abundance of monazite (detrital + metamorphic) was greater than compared to lower-grade samples. As such, this could reflect differences in protolith composition, including trace element composition. However, whole rock geochemistry and the sum total of REE + Y + Th + U (Table 1), do not support this interpretation. In summary, the first option of grain size coarsening with metamorphic grade is the favoured interpretation for explaining the differences in grain-separate yields from low-medium-grade vs. high-grade samples.

Growth of monazite during progressive metamorphism

The aim of this study has been to determine the mechanisms and chemical contributors to monazite growth during prograde metamorphism. Greater than half (54.6%) of all monazite grains in samples for which age data was obtained were found to be detrital in origin. The large quantity of detrital monazite that must have been present in protolith

should therefore be considered as a potential source of monazite-forming elements which might be recrystallised as new monazite during metamorphic processes.

Additionally, apatite was identified, although in low abundance, in several low and medium grade samples, as well as being found as inclusions in monazite grains in high-grade samples STF 21a and STF 21c (Fig. 4 and 5). The textural association between apatite and monazite in high-grade samples provides support that apatite may be breaking down to contribute phosphorus as well as LREEs to the growth of monazite. Within uncertainty, the ages of monazite rims on apatite cores in STF 21c are younger than 1800 Ma, and therefore support the notion of apatite's involvement in monazite growth during metamorphism.

Xenotime was only identified in one sample, STF 21c. However, its presence could indicate that more xenotime is present in the lower-grade samples but is contained within the <70 µm fraction and thus was not readily identifiable, using same logic as above for monazite. Nevertheless, the identification of monazite in the Mt Stafford rocks suggests that xenotime could be another source of elements for the growth of metamorphic monazite.

Previous work by Smith and Barreiro (1990), Pyle and Spear (1999), Wing *et al.* (2003), Kohn and Malloy (2004), Corrie and Kohn (2008), has interpreted that major silicate minerals biotite, muscovite, garnet, plagioclase, aluminosilicates (kyanite or sillimanite), and staurolite were involved in monazite-forming reactions in amphibolite-facies schists. Whereas this has not been able to be quantified in this study, the presence of all of these minerals (andalusite is the dominant aluminosilicate in the samples investigated here) in the Mt Stafford rocks means that their role cannot be discounted. The abundance of REEs in silicate minerals is generally held to be low

(e.g. Bea, 1994). However, since the abundance of these major silicate minerals is vastly greater than that of monazite, the breakdown of any of these minerals with progressive metamorphism could result in appreciable amounts of REEs being released to contribute, along with apatite, xenotime and detrital monazite, to metamorphic monazite growth.

CONCLUSIONS

This study has investigated the growth of prograde monazite using a sequence of contact-metamorphosed pelites and psammities in order to address the incompletely understood reaction mechanisms that produce metamorphic monazite. The main findings of the study are: 1) that the REE content of the rocks is relatively uniform across metamorphic grades and across rock types; 2) that monazite grain-separate yield increases with metamorphic grade, reflecting coarsening of grains with increasing metamorphic grade; 3) that detrital monazite comprises a significant proportion of the total monazite in the rocks, even at granulite-facies conditions, on the basis of U–Pb age data. This is an excellent demonstration of partial melting not resulting in significant dissolution of monazite; 4) that apatite and xenotime are present in lower-grade samples, and in higher-grade samples apatite occurs as inclusions in monazite; 5) that metamorphic monazite growth is probably dominated (or facilitated) by the breakdown of apatite and xenotime and pre-existing monazite but that pre-existing monazite can act as a nucleation site for new (metamorphic) growth of monazite; and 6) that major silicate minerals may also contribute REEs to metamorphic monazite growth due to their vastly greater abundance over monazite, despite probably having quite low REE concentrations. Overall, the role of pre-existing monazite as a major contributor to metamorphic monazite growth indicates that linking monazite growth to specific points

in P - T space (as monitored by changes to silicate mineral assemblage) is not straightforward.

ACKNOWLEDGMENTS

My sincerest thanks to:

Supervisors -

Dr. David Kelsey,
Dr. Caroline Forbes,

Hillgrove Resources and The Playford Memorial Trust,

Adelaide Microscopy -

Dr. Benjamin Wade,
Angus Netting
Aoife McFadden,
Ken Neubauer,

Honours Coordinators-

Dr. Ros King,
Dr. Katie Howard,

Honours and Ph.D Students -

Christopher Kemp,
Jade Anderson,
Kieran Meaney.

REFERENCES

- ANDERSON, J. R., KELSEY, D. E., HAND, M., COLLINS, W. J., 2013. Conductively driven, high-thermal gradient metamorphism in the Anmatjira Range, Arunta region, central Australia. *Journal of Metamorphic Geology*, vol. **31**, p. 1003-1026
- BEA, F., PEREIRA, M. D., STROH, A., 1994. Mineral/leucosome trace-element partitioning in a perilluminous migmatite (a laser ablation-ICP-MS study). *Chemical Geology*, vol. **117**, p. 291-312
- BONYADI, Z., DAVIDSON, G. J., MEHRABI, B., MEFFRE, S., GHAZBAN, F., 2011. Significance of apatite REE depletion and monazite inclusions in the brecciated Se-Chahun iron oxide-apatite deposit, Bafq district, Iran: Insights from paragenesis and geochemistry. *Chemical Geology*, vol. **281**, p. 253-269
- BROWN, M., 1994. The generation, ascent and emplacement of granite magma: the migmatite-to-crustally-derived granite connection in thickened orogens. *Earth-Science Reviews*, vol. **36**, p. 83-130
- CLAUQUÉ-LONG, J., EDGOOSE, C., WORDEN, K., 2008. A correlation of Aileron Province stratigraphy in central Australia. *Precambrian Research*, vol. **166**, p. 230-245
- CORRIE, S. L., KOHN, M. J., 2008. Trace-element distributions in silicates during prograde metamorphic reactions: implications for monazite formation. *Journal of Metamorphic Geology*, vol. **26**, p. 451-464

- CUBLEY, J. F., PATTISON, D. R. M., TINKAM, D. K., FANNING, C. M., U-Pb geochronological constraints of the timing of episodic regional metamorphism and rapid high-T exhumation of the Grand Forks complex, British Columbia. *Lithos*, vol. **156-159**, p. 241-267
- GEBAUER, D., GRÜNENFELDER, M., 1979. U-Th-Pb dating of minerals. In: Jaeger, E., Hunziker, J. C., *Lectures in Isotope Geology*. Springer, Berlin Heidelberg New York, p. 105-131
- GREENFIELD, J. E., CLARKE, G. L., BLAND, M., CLARK, D. J., 1996. *In-situ* migmatite and hybrid diatexite at Mt Stafford, central Australia. *Journal of Metamorphic Geology*, vol. **14**, p. 413-426
- GREENFIELD, J. E., CLARKE, G. L., WHITE, R. W., 1998. A sequence of partial melting reactions at Mt Stafford, central Australia. *Journal of Metamorphic Geology*, vol. **16**, p. 363-378
- GRIFFIN, W., POWELL, W., PEARSON, N., O'REILLY, S., 2008. GLITTER: data reduction software for laser ablation ICP-MS. *Laser Ablation-ICP-MS in the Earth Sciences*. Mineralogical Association of Canada Short Course Series **40**, p. 204-207
- JANOTS, E., BRUNET, F., GOFFÉ, B., POINSSOT, C., BURCHARD, M., CEMIČ, L., 2007. Thermochemistry of monazite-(La) and dissakisite-(La): implications for monazite and allanite stability in metapelites. *Contributions to Mineral Petrology*, vol. **154**, p. 1-14
- JANOTS, E., ENGI, M., BERGER, A., ALLAZ, J., SCHWARZ, J. -O., SPANDLER, C., 2008. Prograde metamorphic sequence of REE minerals in polydeformed rocks of the Central Alps: implications for allanite-monazite-xenotime phase relations from 250 to 610 °C. *Journal of Metamorphic Geology*, vol. **26**, p. 509-526
- KALI, E., LELOUP, P. H., ARNAUD, N., MAHÉO, G., LIU, D., BOUTONNET, E., VAN DER WOERD, J., LIU, X., LIU-ZENG, J., LI, H., Exhumation history of the deepest central Himalayan rocks, Ama Drime range: Key pressure-temperature-deformation-time constraints on orogenic models. *Tectonics*, vol. **29**, p. 1-31
- KELSEY, D. E., POWELL, R., WILSON, C. J. L., STEELE, D. A., 2003. (Th+U)-Pb monazite ages from AL-Mg-rich metapelites, Rauer Group, east Antarctica. *Contributions to Mineral Petrology*, vol. **146**, p. 326-340
- KELSEY, D. E., HAND, M., CLARK, C., WILSON, J. L., 2007. On the application of *in situ* monazite geochronology to constraining *P-T-t* histories in high-temperature (>850 °C) polymetamorphic granulites from Prydz Bay, East Antarctica, *Journal of the Geological Society, London*, vol. **164**, p. 667-683
- KELSEY, D. E., CLARK, C., HAND, M., 2008. Thermobarometric modelling of zircon and monazite growth in melt-bearing systems: examples using model metapelitic and metapsammitic granulites. *Journal of Metamorphic Geology*, vol. **26**, p. 199-212
- KOHN, M. J., MALLOY, M. A., 2004. Formation of monazite via prograde metamorphic reactions among common silicates: Implications for age determinations. *Geochimica et Cosmochimica Acta*, vol. **68**, p. 101-113
- KORHONEN, F. J., SAW, A. K., CLARK, C., BROWN, M., BHATTACHARYA, S., 2011. New constraints on UHT metamorphism in the Eastern Ghats Province through the application of phase equilibria modelling and *in situ* geochronology. *Gondwana Research*, vol. **20**, p. 764-781
- MORRISSEY, L. J., HAND, M., RAIMONDO, T., KELSEY, D. E., Long-lived high-T, low-P granulite facies metamorphism in the Arunta Region, central Australia. *Journal of Metamorphic Geology*, vol. **32**, p. 25-47
- PARRISH, R. R., 1990. U-Pb dating of monazite and its application to geological problems. *Canadian Journal of Earth Sciences*, vol. **27**, p. 1431-1450
- POWELL, R., 1978. Equilibrium thermodynamics in petrology: an introduction, Harper & Row. London, New York. P. 284
- PYLE, J. M., SPEAR, F. S., 1999. Yttrium zoning in garnet: Coupling of major and accessory phases during metamorphic reactions. *Geological Materials Research*, vol. **1**, no. 6, p. 01-49
- RUBATTO, D., WILLIAMS, I. S., BUICK, I. S., 2001. Zircon and monazite response to prograde metamorphism in the Reynolds Range, central Australia. *Contributions to Mineral Petrology*, vol. **140**, p. 458-468

- RUBATTO, D., HERMANN, J., BUICK, I. S., 2006. Temperature and Bulk Composition Control on the Growth of Monazite and Zircon during Low-pressure Anatexis (Mount Stafford, Central Australia). *Journal of Petrology*, vol. **47**, p. 1973-1996
- RUBATTO, D., CHAKRABORTY, S., DASGUPTA, S., 2013. Timescales of crustal melting in the Higher Himalayan Crystallines (Sikkim, Eastern Himalaya) inferred from trace element-constrained monazite and zircon chronology. *Contributions to Mineral Petrology*, vol. **165**, p. 349-372
- SMITH, H. A., BARREIRO, B., 1990. Monazite U-Pb dating of staurolite grade metamorphism in polydeformed schists. *Contributions to Mineral Petrology*, vol. **105**, p. 602-615
- SPEAR, F. S., PYLE, J. M., 2010. Theoretical modelling of monazite growth in a low-Ca metapelite. *Chemical Geology*, vol. **273**, p. 111-119
- STEPANOV, A. S., HERMANN, J., RUBATTO, D., RAPP, R. P., 2012. Experimental study of monazite/melt partitioning with implications for the REE, Th and U geochemistry of crustal rocks. *Chemical Geology*, vol. **300-301**, p. 200-220
- VAN ACHTERBERG, E., RYAN, C. G., JACKSON, S. E., GRIFFIN, W. L., 2001. Data reduction software for ICPMS. In: *Laser-ablation-ICPMS in the earth sciences; principles and applications*. Mineralogical Association of Canada, Ottawa, ON, Canada.
- WARREN, C. J., GRUJIC, D., KELLETT, D. A., COTTLE, J., JAMIESON, R. A., GHALLEY, K. S., Probing the depths of the India-Asia collision: U-Th-Pb monazite chronology of granulites from NW Bhutan. *Tectonics*, vol. **30**, p. 1-24
- WHITE, R. W., POWELL, R., CLARKE G. L., 2003. Prograde Metamorphic Assemblage Evolution during Partial Melting of Metasedimentary Rocks at Low Pressures: Migmatites from Mt Stafford, Central Australia. *Journal of Petrology*, vol. **44**, p. 1937-1960
- WING, B. A., FERRY, J. M., HARRISON, T. M., 2003. Prograde destruction and formation of monazite and allanite during contact and regional metamorphism of pelites: petrology and geochronology. *Contributions to Mineral Petrology*, vol. **145**, p. 228-250
- YAKYMCHUK, C., BROWN, M., Behaviour of zircon and monazite during crustal melting. *Journal of the Geological Society, London*, vol. **171**, p. 465-479

APPENDIX A: WHOLE-ROCK GEOCHEMISTRY

Appendix A

Specimen	SiO2	TiO2	Al2O3	Fe2O3T	MnO	MgO	CaO	Na2O	K2O	P2O5	LOI	Total	Rb	Sr	Y	Zr	V	Ni	Cr	Nb	Ga	Cu	Zn	Co	Ba	La	Ce	U	Th	Sc	Pb	REE+Y+Th+U	Heat Prod.
STF 1	56.95	0.58	22.77	9.00	0.11	2.72	0.48	0.40	5.98	0.14	1.74	100.87	342.1	28	23.4	85	76	46	52	17.6	32.2	38	144	27	804	41	106	0.5	39.0	15	11	209.9	4.35
STF-2a	62.52	0.59	20.30	6.59	0.19	2.13	0.29	0.38	5.92	0.09	1.75	100.75	340.3	185	26.6	156	84	40	73	16.1	30.7	18	100	18	829	40	90	0.7	26.8	12	16	184.1	3.47
STF-2b	55.39	0.61	24.43	8.06	0.13	2.60	0.34	0.62	6.64	0.13	2.06	101.01	380.7	106	34.2	118	92	42	70	16.6	34.2	37	111	17	913	45	108	0.5	33.5	14	17	221.2	4.05
STF 3	74.91	0.46	12.67	4.35	0.06	1.25	0.63	0.86	3.84	0.11	0.71	99.85	235.3	35	23.1	200	47	28	38	14.5	19.9	12	65	11	535	39	70	1.8	34.0	7	9	167.9	3.99
STF 4a	83.20	0.32	8.84	1.77	0.06	0.48	0.66	1.05	2.41	0.11	1.11	100.01	96.4	57	24.7	335	27	16	25	10.0	12.6	8	27	1	487	46	80	3.2	37.0	2	14	190.9	4.42
STF-5	57.95	0.60	22.65	7.92	0.09	2.38	0.25	0.81	6.15	0.14	0.66	99.60	339.1	49	28.2	102	77	45	64	16.1	32.7	21	123	23	911	42	106	0.5	35.1	15	19	211.8	4.08
STF-6	56.21	0.66	24.00	7.59	0.12	2.39	0.32	0.98	6.49	0.13	1.45	100.34	368.2	95	29.3	119	89	53	78	17.0	34.5	16	119	22	1002	42	119	1.1	33.7	16	1	225.1	4.25
STF-7	62.28	0.61	19.99	6.05	0.08	1.97	0.30	1.20	6.34	0.14	0.79	99.75	280.2	60	28.6	151	65	38	61	15.6	29.1	18	97	16	1326	45	112	1.5	30.3	12	22	217.4	4.09
STF-8	77.94	0.39	11.23	3.79	0.11	1.05	0.78	0.72	3.12	0.10	0.85	100.08	172.2	192	20.1	245	44	25	48	12.0	16.9	14	63	7	719	37	87	0.9	31.0	4	15	176.0	3.31
STF-9	54.83	0.64	26.49	6.32	0.09	2.11	0.37	1.44	6.46	0.16	0.89	99.80	366.1	42	37.0	101	86	47	72	18.3	41.2	17	89	17	1415	48	140	5.0	33.0	18	13	263.0	5.52
STF-10b	75.16	0.47	13.17	4.48	0.13	1.35	0.71	0.74	3.25	0.11	0.89	100.46	161.8	121	24.1	251	60	31	59	13.5	20.2	16	73	11	521	41	84	1.2	33.7	6	13	184.0	3.65
STF-11	71.74	0.56	13.98	5.25	0.08	1.58	0.53	1.03	4.37	0.11	1.01	100.24	232.7	167	12.8	184	67	32	76	16.5	22.0	19	89	14	735	28	66	0.5	23.5	9	19	130.8	2.84
STF-12	58.64	0.57	21.63	6.63	0.07	1.95	0.31	1.58	7.22	0.13	1.57	100.30	432.0	158	19.1	119	81	41	89	14.9	28.9	24	105	17	1382	38	102	0.5	22.2	12	24	181.8	3.30
STF-13	70.01	0.58	14.39	5.71	0.06	1.60	0.74	1.54	4.38	0.10	1.07	100.18	273.9	201	14.1	187	72	35	79	15.7	21.0	18	86	14	926	29	62	0.5	19.5	8	20	125.1	2.53
STF-16a	55.53	0.59	24.73	7.83	0.06	2.03	0.21	1.23	6.62	0.13	0.72	99.68	407.7	49	28.5	92	69	38	60	16.7	34.5	41	115	18	1060	42	109	0.5	35.2	13	23	215.2	4.18
STF-16b	64.38	0.58	19.16	6.22	0.09	1.93	0.22	0.90	5.57	0.13	1.30	100.48	349.5	94	19.6	169	76	38	68	17.7	28.2	7	93	14	706	35	82	0.5	29.6	8	19	166.7	3.54
STF-17a	74.46	0.47	13.46	4.42	0.06	1.13	0.11	0.46	4.33	0.09	1.08	100.07	250.2	90	15.9	235	53	27	64	12.1	20.7	15	69	9	665	37	73	0.6	30.5	5	28	157.0	3.41
STF-17b	70.45	0.60	15.44	5.85	0.07	1.67	0.19	0.51	4.38	0.12	1.07	100.35	273.7	80	16.7	200	69	41	81	18.6	24.7	16	80	18	677	31	69	0.5	26.0	10	16	143.2	3.03
STF-18a	60.92	0.52	21.42	4.72	0.07	1.46	0.36	1.59	8.02	0.14	0.47	99.69	443.3	68	16.5	95	54	35	67	14.6	28.2	6	102	8	1029	33	76	0.5	22.5	8	36	148.5	3.48
STF-18b	56.69	0.58	24.13	6.50	0.07	2.06	0.19	1.27	7.42	0.12	0.59	99.62	408.4	44	28.6	99	65	43	67	13.8	33.7	19	114	17	926	39	89	1.8	32.4	10	34	190.8	4.57
STF-18c dark	66.39	0.62	18.68	8.15	0.08	2.54	0.25	0.54	1.85	0.10	1.42	100.62	109.0	49	57.0	221	79	62	88	14.9	32.8	78	92	29	236	37	87	0.5	36.4	13	10	217.9	3.34
STF-18c light	56.96	0.45	24.59	6.86	0.08	2.06	0.21	1.12	6.52	0.13	1.21	100.19	379.2	75	33.9	125	79	54	86	16.5	36.8	33	138	20	923	39	95	0.5	30.6	13	33	199.0	3.81
STF-18d	70.43	0.59	15.86	6.17	0.07	1.83	0.22	0.66	3.26	0.13	0.49	99.71	167.8	32	28.5	198	53	40	39	16.8	24.9	12	75	19	603	39	80	1.7	42.2	8	17	191.4	4.48
STF-20	79.59	0.44	9.81	3.61	0.06	1.13	0.96	1.41	2.69	0.11	0.73	100.54	140.3	96	18.7	349	45	26	56	13.3	17.1	8	47	6	517	38	83	1.3	38.8	4	14	179.8	3.97
STF-21a	74.95	0.51	12.89	4.28	0.06	1.19	1.00	1.08	2.98	0.11	0.50	99.55	159.9	67	20.4	234	45	26	50	15.2	19.2	6	64	9	504	39	64	1.3	29.1	8	18	153.8	3.27
STF-21b	76.43	0.43	12.43	4.22	0.05	1.19	0.39	0.75	3.20	0.11	0.52	99.72	154.3	42	20.0	213	39	27	34	11.4	18.6	12	63	8	521	34	69	2.6	36.6	6	8	162.2	4.34
STF-21c	58.82	0.71	22.74	6.79	0.09	2.07	0.33	1.22	6.23	0.12	0.60	99.72	343.0	75	24.1	128	72	46	68	19.2	33.5	10	111	17	798	37	78	1.6	31.8	11	19	172.5	4.22
STF-22	74.64	0.31	13.62	2.49	0.05	0.71	1.15	1.94	4.23	0.13	0.81	100.08	258.9	102	9.5	196	30	16	32	10.8	20.8	12	37	1	462	29	56	0.5	25.3	3	17	120.3	2.95
STF-24	73.20	0.38	12.25	4.10	0.08	1.41	2.59	2.06	3.52	0.10	0.86	100.55	208.3	107	18.3	277	46	24	40	9.8	17.4	11	45	8	412	32	76	0.5	25.2	7	6	152.0	2.80
STF-25	77.86	0.25	11.15	2.18	0.04	0.30	0.86	1.77	4.74	0.11	0.79	100.05	550.3	42	60.1	248	17	9	11	12.6	17.9	11	33	<1	201	36	71	1.8	65.1	3	21	234.0	6.57
STF-26a	73.69	0.55	12.78	6.61	0.11	1.83	0.47	0.59	2.36	0.10	1.25	100.34	119.4	57	23.5	260	64	38	81	13.8	20.1	7	134	21	516	40	83	0.5	25.3	17	14	172.3	2.59
STF-26b	74.34	0.57	12.91	6.02	0.09	1.64	1.01	0.94	1.93	0.10	0.09	99.64	91.5	32	25.3	206	54	33	49	12.1	20.5	6	117	18	472	39	73	1.3	29.2	12	17	167.8	3.08
STF-27	74.63	0.54	12.20	4.23	0.08	1.25	0.93	1.39	3.22	0.11	1.63	100.21	137.1	210	19.1	340	57	29	69	12.7	18.3	8	64	9	903	39	79	1.6	31.9	5	11	170.6	3.64
STF-28 dark	50.47	1.31	26.27	13.34	0.09	4.12	0.11	0.12	0.57	0.06	1.93	98.39	58.7	19	31.7	178	178	71	147	32.2	42.0	13	137	53	62	50	111	1.2	48.0	23	<1	241.9	4.23
STF-28 light	56.79	0.60	23.80	7.48	0.05	2.26	0.26	1.05	6.94	0.12	1.38	100.73	322.8	138	20.3	126	88	55	95	14.1	30.8	8	115	21	1378	46	120	0.5	30.6	11	27	217.4	3.89
STF-29	79.91	0.43	9.75	3.21	0.08	0.84	1.44	1.46	2.03	0.09	0.65	99.89	75.5	196	18.9	326	39	20	61	10.2	15.3	7	41	4	648	43	79	0.5	23.7	4	15	165.1	2.40
STF 30	55.10	0.59	24.06	7.30	0.62	2.36	1.06	2.83	4.67	0.13	2.23	100.95	224.1	216	38.3	84	76	49	60	16.7	32.7	7	160	23	987	46	101	1.1	34.0	10	32	220.4	3.91
STF 31a	77.69	0.38	11.30	3.06	0.06	0.92	0.62	1.48	3.36	0.10	1.34	100.31	182.4	93	21.5	222	44	20	43	13.0	17.6	14	51	4	774	35	63	4.9	34.0	6	17	158.4	4.96
STF 31b	71.37	0.56	14.23	5.03	0.06	1.64	0.15	0.24	4.88	0.11	2.44	100.71	330.2	17	37.5	273	62	31	43	15.7	23.9	17	87	8	700	55	104	2.4	48.0	9	14	246.9	5.48
STF 31af	77.28	0.38	10.90	3.21	0.24	0.95	0.89	1.84	3.12	0.11	1.17	100.09	166.7	141	27.2	229	42	19	35	12.0	17.5	13	51	3	1118	38	82	5.2	33.0	5	16	185.4	4.93
STF-32	81.02	0.34	8.72	1.86	0.03	0.51	0.27	0.78	5.31	0.11	0.82	99.77	279.8	65	9.9	340	30	15	46	11.8	10.2	10	15	<1	849	30	100	0.9	36.9	2	3	177.7	4.19
STF-33	76.73	0.37	1																														

APPENDIX B: ELECTRON MICROPROBE ANALYSES

Appendix B

Data ID	Sample #	Run #	Grain ID	Zone	Lithology	Min. ID	Pb206/207	Source	Age Group	Si_wt%	P_wt%	La_wt%	Ce_wt%	Ca_wt%	O_wt%	Zr_wt%	Pb_wt%	Th_wt%	U_wt%	Y_wt%	Pr_wt%	
1	STF 01	1	1	1	Pelite	Monazite	1700.5	Metam.	1700-1725	0.764809	13.3286	9.82593	22.4645	0.71246	28.0202	0.071805	0.58101	9.0964	0.177514	1.99711	2.16082	
2	STF 01	1	2	1	Pelite	Monazite	1709.1	Metam.	1700-1725	0.754252	13.2444	10.2429	23.7379	0.458798	27.8715	0.096622	0.463289	7.51721	0.100501	1.69042	2.24633	
3	STF 01	1	3	1	Pelite	Monazite	1779.7	Metam.	1775-1800	0.097704	14.6024	13.1998	25.4666	0.262544	28.9998	0.095396	0.068105	0.109414	0.273118	3.51723	2.26971	
4	STF 01	1	4	1	Pelite	Monazite	0.1	Unkn.	0	0.861624	13.2862	9.08406	21.0268	0.863955	28.1178	0.081944	0.787585	0.51103	0.275804	2.64914	2.08685	
5	STF 01	1	5	1	Pelite	Monazite	0.1	Unkn.	0	0.835866	13.2554	10.1742	23.4019	1.59862	28.2125	0.066511	0.376853	7.86589	0.084976	1.39014	2.18986	
6	STF 01	1	6	1	Pelite	Monazite	1853.9	Detri.	1850-1875	0.818005	13.1736	10.5933	24.4783	0.409259	27.9212	0.084701	0.445545	7.08522	0.129376	1.76751	2.1933	
7	STF 01	1	7	1	Pelite	Monazite	1764.3	Metam.	1700-1725	0.724094	14.4351	12.2425	24.4024	0.360739	28.8079	0.073979	0.213225	0.410958	0.715308	3.58925	2.2818	
8	STF 01	1	8	1	Pelite	Monazite	1775.9	Metam.	1775-1800	0.186707	14.5446	12.8753	25.7407	0.31186	28.7833	0.093754	0.202296	0.605238	0.61947	1.64612	2.32067	
9	STF 01	2	1	1	Pelite	Monazite	1700.5	Metam.	1700-1725	0.74275	13.4582	9.58809	21.9517	0.6462	28.1276	0.085187	0.596918	8.82453	0.231822	2.43583	2.18376	
10	STF 01	2	2	1	Pelite	Monazite	1709.1	Metam.	1700-1725	0.695562	13.3473	10.2517	23.4614	0.629256	27.9573	0.083359	0.503682	7.67649	0.143231	1.95617	2.11948	
11	STF 01	2	3	1	Pelite	Monazite	1779.7	Metam.	1775-1800	0.514461	13.9578	13.4919	25.5148	0.235583	28.3033	0.07504	0.0779	0.16719	0.381335	2.46521	2.19106	
12	STF 01	2	4	1	Pelite	Monazite	0.1	Unkn.	0	1.11141	13.1415	10.3497	23.3146	0.471181	28.3667	0.634058	0.171391	7.48813	0.115661	2.65885	2.14352	
13	STF 01	2	5	1	Pelite	Monazite	0.1	Unkn.	0	1.35079	12.4019	9.04608	20.9462	0.64167	27.4646	0.08468	0.923786	12.6933	0.387548	1.77047	2.06489	
14	STF 01	2	6	1	Pelite	Monazite	1853.9	Detri.	1850-1875	0.674424	13.2954	10.2874	24.1008	0.437748	27.8405	0.075699	0.440302	6.7484	0.106396	1.64902	2.25668	
15	STF 01	2	7	1	Pelite	Monazite	1764.3	Metam.	1700-1725	0.108563	14.1127	12.6031	24.2713	0.413121	28.2815	0.074558	0.17339	1.39556	0.363631	3.40256	2.19015	
16	STF 01	2	8	1	Pelite	Monazite	1775.9	Metam.	1775-1800	0.262006	13.2331	11.4791	23.2621	0.448588	26.9222	0.067994	0.167346	6.08346	0.509155	3.45471	2.20742	
17	STF 01	2	9	1	Pelite	Monazite	1797.3	Metam.	1775-1800	0.18754	14.4954	13.5378	25.892	0.194362	28.757	0.100401	0.032056	0.05465	0.237709	2.29675	2.39957	
18	STF 03	1	1	1	Psammite	Monazite	1876.7	Detri.	1875-1900	0.338516	13.7394	11.4383	24.0917	0.651525	27.8325	0.082707	0.397236	4.88813	0.208106	0.416442	2.41674	
19	STF 03	1	2	1	Psammite	Monazite	1790.6	Metam.	1775-1800	0.979167	13.0451	14.0449	25.4211	0.255245	27.8402	0.073177	0.549655	6.62894	0.283281	1.12056	2.05306	
20	STF 03	1	3	1	Psammite	Monazite	1858.8	Detri.	1850-1875	0.552501	13.6496	11.5259	23.7443	0.68077	28.0093	0.09273	0.460037	6.44919	0.071027	0.740255	2.21466	
21	STF 03	1	4	1	Psammite	Monazite	1844.3	Detri.	1825-1850	1.46684	12.3946	10.6986	22.9664	0.365619	27.0696	0.088097	0.539862	6.88984	0.172356	0.621637	2.19607	
22	STF 03	1	5	1	Psammite	Monazite	1850.8	Detri.	1850-1875	0.650889	13.6056	11.9311	24.8047	0.333317	28.1435	0.09385	0.449548	5.79018	0.11315	0.500011	2.25525	
23	STF 03	1	6	1	Psammite	Monazite	1822.4	Detri.	1800-1825	0.271152	14.1986	13.3337	26.9231	0.082399	28.4664	0.099564	0.094151	2.11414	0.019245	0.407823	2.4314	
24	STF 03	1	7	1	Psammite	Monazite	1786.2	Metam.	1775-1800	0.950459	13.0488	9.316	25.4753	0.203342	27.84	0.075507	0.530462	6.80358	0.233682	1.11711	2.08472	
25	STF 03	1	8	1	Psammite	Monazite	1782.4	Metam.	1775-1800	0.898464	13.2963	14.1272	26.597	0.196324	28.1613	0.070369	0.47312	6.22453	0.201056	1.11803	2.09294	
26	STF 03	1	9	1	Psammite	Monazite	1799.5	Metam.	1775-1800	1.0025	12.9426	13.793	25.5167	0.262346	27.7513	0.086134	0.618373	1.7651	0.284874	1.173	2.00285	
27	STF 03	1	10	1	Psammite	Monazite	0.1	Unkn.	0	0.547644	13.5662	9.87199	20.2638	1.85001	28.271	0.076521	1.0225	12.1676	0.395511	1.55348	1.7779	
28	STF 03	1	11	1	Psammite	Monazite	1894.2	Detri.	1875-1900	0.674891	13.1397	12.1035	24.9558	0.189235	27.3979	0.076919	0.327445	5.94411	0.028455	0.366685	2.30914	
29	STF 03	1	12	1	Psammite	Monazite	1850.8	Detri.	1850-1875	0.569218	12.8751	10.2999	22.566	1.33278	27.059	0.141768	0.593215	8.89946	0.069614	0.740242	2.01856	
30	STF 03	2	1	1	Psammite	Monazite	1876.7	Detri.	1875-1900	0.397944	13.798	12.2743	25.5616	0.177374	27.9983	0.097367	0.211044	3.70412	0.050283	0.602179	2.3086	
31	STF 03	2	2	1	Psammite	Monazite	1844.3	Detri.	1825-1850	0.686	13.4145	11.185	22.1555	1.27635	28.1195	0.09849	0.948207	12.1034	0.354402	1.49526	1.84508	
32	STF 03	2	3	1	Psammite	Monazite	1786.2	Metam.	1775-1800	0.3911	13.6082	12.8072	20.7016	0.525927	27.9124	0.09456	0.392391	4.21797	0.058407	0.540064	2.20987	
33	STF 03	2	3	2	1	Psammite	Monazite	0.1	Unkn.	0	0.261693	12.997	11.4512	24.9071	0.571883	26.2466	0.068389	0.684659	5.18365	0.094283	1.054099	1.85917
34	STF 03	2	3	3	1	Psammite	Monazite	1928.2	Detri.	1925-1950	0.475306	13.4006	9.95903	23.2791	0.77246	27.2494	0.091317	0.602213	7.40984	0.11674	0.314446	2.22507
35	STF 08	1	1	2a	Psammite	Monazite	1783.4	Metam.	1775-1800	0.293212	13.4933	10.8456	22.1525	0.774294	27.1041	0.091008	0.372083	3.44794	0.305172	1.2506	2.21176	
40	STF 08	1	5	2a	Psammite	Monazite	1841.9	Detri.	1825-1850	0.910065	13.1922	8.81951	20.9429	0.651417	28.0144	0.06459	0.824088	9.77608	0.318278	1.31975	2.16485	
42	STF 08	1	7	2a	Psammite	Monazite	1881.2	Detri.	1875-1900	0.475419	13.8144	8.1359	19.4704	1.87317	28.2995	0.07673	1.09168	12.6511	0.468883	1.89789	1.96059	
43	STF 08	1	8	2a	Psammite	Monazite	1796.7	Metam.	1775-1800	0.344944	14.0716	12.477	22.7251	0.989754	28.4772	0.09368	0.518135	5.85475	0.376552	2.3098	1.96178	
44	STF 08	1	9	2a	Psammite	Monazite	0.1	Unkn.	0	0.733217	13.3249	8.34178	17.1263	2.2411	28.0661	0.078409	1.37956	16.0724	0.596117	2.45327	1.6055	
45	STF 08	1	10	2a	Psammite	Monazite	1991.8	Detri.	1975-2000	0.160812	13.9248	13.2572	24.6601	0.496242	27.6814	0.064794	0.243703	3.19671	0.102496	1.74403	2.04408	
46	STF 08	1	11	2a	Psammite	Monazite	1718.1	Metam.	1700-1725	0.722901	14.1277	8.63472	17.8955	1.96561	29.1098	0.092348	1.21638	15.2612	0.451748	2.62013	1.61897	
48	STF 08	1	13	2a	Psammite	Monazite	1752.8	Metam.	1700-1725	0.252295	14.2633	9.27244	22.2734	0.722831	28.3599	0.072493	0.402935	4.35569	0.341385	1.93366	2.46374	
49	STF 08	1	14	2a	Psammite	Monazite	1788.3	Metam.	1775-1800	1.54942	13.0163	10.9246	22.1276	1.03195	28.3747	0.075166	0.520697	6.98372	0.368421	2.1861	2.07018	
50	STF 08	1	15	2a	Psammite	Monazite	1844.2	Detri.	1825-1850	0.721822	13.6001	10.2953	22.738	0.706682	28.2072	0.081763	0.633674	8.3769	0.229769	1.65103	2.11095	
51	STF 08	2	1	2a	Psammite	Monazite	1783.4	Metam.	1775-1800	0.356605	14.2087	11.4343	22.9334	0.979109	28.9085	0.067099	0.606714	6.35553	0.493626	2.90081	2.09253	
54	STF 08	2	4	2a	Psammite	Monazite	1826.1	Detri.	1825-1850	0.461706	11.0775	11.3063	22.6535	0.675409	24.2649	0.058449	0.481123	5.99157	0.231374	1.41764	2.1021	
55	STF 08	2	5	2a	Psammite	Monazite	1841.9	Detri.	1825-1850	0.934328	13.1777	8.7373	21.1258	0.651852	28.1074	0.083298	0.373104	10.0903	0.336116	3.33701	2.06266	
56	STF 08	2	6	2a	Psammite	Monazite	1907.9	Detri.	1900-1925	0.179622	13.9416	11.5768	22.4488	0.995184	27.9248	0.104308	0.485156	5.16692	0.422341	1.38788	1.2109	
57	STF 08	2	7	2a	Psammite	Monazite	1881.2	Detri.	1875-1900	0.585719	13.7846	8.10277	19.2718	1.87663	28.5159	0.080598	1.09193	13.1076	0.466277	1.90556	1.94412	
58	STF 08	2	8	2a	Psammite	Monazite	1796.7	Metam.	1775-1800	0.269241	14.1989	13.2555	23.6848	0.993717	28.6236	0.096234	0.48486	5.03869	0.451283	2.28676	1.93668	
59	STF 08	2	9	2a	Psammite	Monazite	0.1	Unkn.	0	0.760242	13.4557	7.92466	16.687	2.31263	28.4208	0.061176	1.50706	17.1843	0.613215	2.72227	1.58729	
60	STF 08	2	10	2a	Psammite	Monazite	1991.8	Detri.	1975-2000	0.115733	12.9918	11.6895	22.4551	0.981392	26.4136	0.056364	0.392829	4.4335				

Appendix B

126	STF 21a	1	58	2b	Pelite	Monazite	1779.1	Metam.	1775-1800	0.24934	13.9709	12.4433	23.9209	0.831123	28.2725	0.093707	0.376793	5.02863	0.120059	1.82183	2.09448
127	STF 21a	1	59	2b	Pelite	Monazite	1750.8	Metam.	1750-1775	0.342595	13.531	11.4152	22.0326	0.857413	27.5793	0.084344	0.516138	6.44792	0.214905	2.36122	2.04286
128	STF 21a	1	60	2b	Pelite	Monazite	1775.8	Metam.	1775-1800	0.242828	13.9795	11.1468	22.1983	1.02309	28.2842	0.077745	0.532892	6.42496	0.303458	2.68993	2.06015
129	STF 21a	2	1	2b	Pelite	Monazite	0	Unkn.	0	0.140998	14.13	11.7854	22.2432	1.20714	28.4873	0.073375	0.856618	5.3941	1.24149	3.02642	1.9235
130	STF 21a	2	2	2b	Pelite	Monazite	0	Unkn.	0	0.284868	14.1861	9.61207	21.5383	1.33307	28.6165	0.081503	0.791118	8.65694	0.431083	1.88717	2.10297
131	STF 21a	2	3	2b	Pelite	Monazite	0	Unkn.	0	0.200233	14.1822	12.1572	24.5302	0.724441	28.4437	0.080284	0.378569	4.98887	0.074831	0.961238	2.26813
132	STF 21a	2	4	2b	Pelite	Monazite	0	Unkn.	0	0.556785	14.4859	10.3103	22.8694	0.73706	29.134	0.090338	0.488411	7.05465	0.051289	2.14894	2.08843
133	STF 21a	2	5	2b	Pelite	Monazite	0	Unkn.	0	0.275539	14.0548	11.0647	23.7311	0.938308	28.4967	0.10134	0.481592	5.75124	0.190931	2.08008	2.1592
134	STF 21a	2	6	2b	Pelite	Monazite	0	Unkn.	0	0.297256	13.5712	11.3519	23.5352	0.900313	27.7949	0.084979	0.465005	5.75668	0.099647	1.77226	2.1471
135	STF 21a	2	7	2b	Pelite	Monazite	0	Unkn.	0	0.370656	13.8991	11.9711	24.0055	0.628648	28.3845	0.073278	0.502025	5.21718	0.37157	2.4134	2.13376
136	STF 21a	2	8	2b	Pelite	Monazite	0	Unkn.	0	0.468025	14.3095	12.0075	23.8885	1.01195	28.9502	0.085118	0.665558	4.12266	0.985916	1.78831	2.05194
137	STF 21a	2	9	2b	Pelite	Monazite	0	Unkn.	0	0.6663	13.3818	12.703	22.9696	0.825169	28.0757	0.08228	0.742332	8.31459	0.289969	2.12897	1.79116
138	STF 21a	2	10	2b	Pelite	Monazite	0	Unkn.	0	0.171151	14.4139	9.55056	21.0973	1.54026	28.9109	0.070987	0.963266	7.60371	1.19762	2.71456	1.96622
139	STF 21a	2	11	2b	Pelite	Monazite	0	Unkn.	0	0.222321	14.2188	11.4088	22.8756	1.04578	28.6945	0.080976	0.505483	5.66327	0.224455	2.66776	2.06028
140	STF 21a	2	12	2b	Pelite	Monazite	0	Unkn.	0	0.482827	13.7361	12.0274	24.5811	0.782821	28.3093	0.093816	0.493675	6.75495	0.113971	1.28688	2.07433
141	STF 21a	2	13	2b	Pelite	Monazite	0	Unkn.	0	0.381753	13.7451	10.5474	22.7245	0.958576	28.096	0.072595	0.591021	7.1515	0.20276	1.83102	2.11229
142	STF 21a	2	14	2b	Pelite	Monazite	0	Unkn.	0	0.425552	13.751	10.7736	22.719	1.17032	28.2738	0.097993	0.758946	3.83552	0.410977	1.48916	2.15839
143	STF 21a	2	15	2b	Pelite	Monazite	0	Unkn.	0	0.168067	14.3523	11.1455	22.4621	0.926703	28.8964	0.090638	0.519263	4.28151	0.538255	4.17482	2.03948
144	STF 21a	2	16	2b	Pelite	Monazite	0	Unkn.	0	0.227216	14.1191	11.3333	23.245	0.939916	28.5744	0.087582	0.472221	5.85324	0.264871	2.92372	2.0373
145	STF 21a	2	17	2b	Pelite	Monazite	0	Unkn.	0	0.352613	14.0499	11.587	23.264	0.82952	28.3918	0.107443	0.378304	4.57865	0.299307	2.37304	2.09242
146	STF 21a	2	18	2b	Pelite	Monazite	0	Unkn.	0	0.204802	14.0913	11.9176	23.17	0.764871	28.5075	0.085826	0.410457	5.17767	0.179143	3.11337	2.07786
147	STF 21a	2	19	2b	Pelite	Monazite	0	Unkn.	0	0.216881	14.2613	11.9072	23.317	0.745234	28.7442	0.075538	0.389532	5.07797	0.196457	3.13054	2.06804
148	STF 21a	2	20	2b	Pelite	Monazite	0	Unkn.	0	0.264113	14.0334	12.4397	24.1668	0.757595	28.477	0.113518	0.386975	5.16221	0.139374	2.24348	2.02042
149	STF 21a	2	21	2b	Pelite	Monazite	0	Unkn.	0	0.67456	13.3285	12.1446	25.9885	0.196519	27.8847	0.088594	0.364105	4.66202	0.145228	1.33222	2.34412
150	STF 21a	2	22	2b	Pelite	Monazite	0	Unkn.	0	0.182032	13.9655	12.574	24.2758	0.727894	28.2766	0.077133	0.348712	4.18438	0.274307	2.80959	2.08472
151	STF 21a	2	23	2b	Pelite	Monazite	0	Unkn.	0	0.432064	13.8886	8.36437	19.9568	1.55709	28.3474	0.085454	1.09793	9.84968	1.00519	1.44121	2.10365
152	STF 21a	2	24	2b	Pelite	Monazite	0	Unkn.	0	0.422407	13.1329	11.7334	24.0437	0.924578	27.164	0.092669	0.474828	6.25851	0.142426	0.660471	2.16657
153	STF 21a	2	25	2b	Pelite	Monazite	0	Unkn.	0	0.282201	13.7076	12.477	24.3581	0.754403	27.8948	0.07933	0.353294	5.23065	0.051311	1.00596	2.18202
154	STF 21a	2	26	2b	Pelite	Monazite	0	Unkn.	0	0.237619	13.9712	10.3001	21.8215	1.29859	28.2642	0.077598	0.689089	6.95125	0.542151	1.63641	2.06603
155	STF 21a	2	27	2b	Pelite	Monazite	0	Unkn.	0	0.142153	14.2873	10.2102	21.4662	1.44385	28.6547	0.087948	0.780051	8.68348	0.879849	2.34381	2.05427
156	STF 21a	2	28	2b	Pelite	Monazite	0	Unkn.	0	0.233622	14.1614	11.5699	21.8224	1.13311	28.5397	0.080896	0.693715	5.3767	0.636989	2.86448	2.00204
157	STF 21a	2	29	2b	Pelite	Monazite	0	Unkn.	0	0.173449	13.9906	10.9244	22.5414	1.19454	27.9567	0.105553	0.643388	5.79882	0.632365	1.0333	2.07103
158	STF 21a	2	30	2b	Pelite	Monazite	0	Unkn.	0	1.48467	12.0787	10.0749	22.2504	0.182796	27.1426	0.081055	0.931303	11.1274	0.406372	1.6344	2.04867
162	STF 21a	2	34	2b	Pelite	Monazite	0	Unkn.	0	0.39584	13.1359	9.36612	20.4827	1.17785	26.9276	0.085	0.675619	8.23213	0.223787	2.53191	1.95475
163	STF 21a	2	35	2b	Pelite	Monazite	0	Unkn.	0	0.215882	14.2621	11.7446	22.5919	1.04041	28.6917	0.081712	0.63622	6.02137	0.558598	2.6449	2.0036
164	STF 21a	2	36	2b	Pelite	Monazite	0	Unkn.	0	0.114366	14.0644	12.0944	24.8971	1.11021	28.2329	0.085956	0.711494	4.03613	1.23126	1.98433	2.17378
165	STF 21a	2	37	2b	Pelite	Monazite	0	Unkn.	0	0.849749	12.8783	11.6084	22.0733	1.13121	27.7068	0.082352	0.865649	11.5489	0.264932	1.85904	1.79898
166	STF 21a	2	38	2b	Pelite	Monazite	0	Unkn.	0	0.242329	13.9011	10.7254	22.5338	0.965021	28.2867	0.076187	0.517762	6.21555	0.190714	2.92394	2.10332
167	STF 21a	2	39	2b	Pelite	Monazite	0	Unkn.	0	0.251161	13.6299	11.4255	23.0956	0.756004	27.5554	0.067473	0.382043	4.92451	0.122154	2.8137	1.79088
168	STF 21a	2	40	2b	Pelite	Monazite	0	Unkn.	0	0.794685	13.3194	9.10839	22.522	0.952089	27.8229	0.09778	0.806761	10.4773	0.082048	0.140755	2.30826
169	STF 21a	2	41	2b	Pelite	Monazite	0	Unkn.	0	0.410305	13.6921	10.8995	23.656	1.14791	28.4761	0.07412	0.727535	7.89537	0.221822	1.1816	2.14297
170	STF 21a	2	42	2b	Pelite	Monazite	0	Unkn.	0	0.261874	14.0913	11.9832	24.7282	0.781747	28.6156	0.074117	0.456977	5.75858	0.088414	1.77988	2.23668
171	STF 21b	1	1	2b	Psammite	Monazite	1784.6	Metam.	1775-1800	0.180985	14.1353	11.3862	23.4153	0.876347	28.4102	0.077873	0.477029	5.66449	0.307787	2.57595	2.01832
172	STF 21b	1	2	2b	Psammite	Monazite	1842	Detri.	1825-1850	0.418542	13.7079	11.1021	23.62	0.828224	28.1433	0.08262	0.590905	5.79856	0.100337	0.987607	2.11388
173	STF 21b	1	3	2b	Psammite	Monazite	1782.6	Metam.	1775-1800	0.343996	13.8369	10.7485	22.969	0.923298	28.2192	0.074201	0.576665	8.03489	0.158053	1.45754	2.15912
174	STF 21b	1	4	2b	Psammite	Monazite	1942.6	Detri.	1925-1950	0.193178	14.1471	11.7476	24.2153	0.823846	28.5056	0.08124	0.524465	5.05249	0.390136	1.95855	2.11161
175	STF 21b	1	5	2b	Psammite	Monazite	1858	Detri.	1850-1875	0.232269	14.1237	11.5427	22.9947	0.645186	28.3675	0.082223	0.362969	4.78415	0.087158	1.61264	2.16482
176	STF 21b	1	6	2b	Psammite	Monazite	1862.3	Detri.	1850-1875	0.168819	14.0858	11.2885	22.0947	0.866299	28.2322	0.077343	0.455428	5.23931	0.308607	2.75006	2.03911
177	STF 21b	1	7	2b	Psammite	Monazite	1864.7	Detri.	1850-1875	0.179555	14.2535	11.3003	23.5749	0.859604	28.6833	0.073748	0.452144	5.62784	0.309135	2.64284	2.09759
178	STF 21b	1	8	2b	Psammite	Monazite	1847.9	Detri.	1825-1850	0.078226	14.1806	11.2341	22.5357	1.00853	28.3649	0.083081	0.614468	4.32707	0.933685	3.05931	1.97847
179	STF 21b	1	9	2b	Psammite	Monazite	1828.5	Detri.	1825-1850	0.268995	14.0375	11.6356	23.4297	0.982601	28.353	0.072318	0.570263	6.47023	0.371031	1.80797	2.07615
180	STF 21b	1	10	2b	Psammite	Monazite	1864.8	Detri.	1805-1875	0.0956314	14.378	11.848	22.3425	1.25154	28.6798	0.058928	0.807563	5.65787	1.15843	2.87143	1.85288
181	STF 21b	1	11	2b	Psammite	Monazite	1811.1	Detri.	1800-1825	0.17703	14.068	11.4902	24.066	0.861673	28.3913	0.058238	0.50095	5.62675	0.299329	2.38997	2.00728
182	STF 21b	1	12	2b	Psammite	Monazite	1887.6	Detri.	1850-1875	0.088774	14.3359	11.5796	22.4963	0.98159	28.5913	0.096025					

245	STF 21b	1	75	2b	Psammite	Monazite	1848.6	Detri.	1825-1850	0.594984	13.5658	9.96703	22.0522	1.12795	28.1825	0.06645	0.772258	10.8044	0.082856	1.29337	1.98746
246	STF 21b	1	76	2b	Psammite	Monazite	1839.9	Detri.	1825-1850	0.264325	13.7066	9.7486	21.4173	1.20591	28.0094	0.069228	0.761539	9.57384	0.654453	2.82653	1.89272
247	STF 21b	1	77	2b	Psammite	Monazite	1892.6	Detri.	1875-1900	0.181444	14.1819	9.1555	21.3864	1.45905	28.6265	0.080328	0.292435	7.81714	1.02035	3.02663	0.07115
248	STF 21b	1	78	2b	Psammite	Monazite	1777.8	Metam.	1775-1800	0.259261	14.0778	11.4851	24.0685	0.766663	28.4284	0.080593	0.437487	5.18489	0.25364	1.99463	0.27409
249	STF 21b	1	79	2b	Psammite	Monazite	1903.4	Detri.	1900-1925	0.924776	12.9526	9.9806	22.1943	0.772372	27.749	0.092937	0.826888	11.0906	0.073164	1.12515	1.95189
250	STF 21b	1	80	2b	Psammite	Monazite	1855	Detri.	1850-1875	0.099701	14.248	11.3767	22.8741	0.942479	28.4994	0.06798	0.553875	4.8737	0.563872	3.1805	0.32529
251	STF 21b	1	81	2b	Psammite	Monazite	1818.6	Detri.	1800-1825	0.158604	14.195	11.5108	23.8951	0.915329	28.5774	0.075891	0.484829	5.62187	0.309288	2.37191	0.98979
252	STF 21b	1	82	2b	Psammite	Monazite	1847.4	Detri.	1825-1850	0.170734	13.9875	11.6838	24.8064	0.763042	28.1411	0.090578	0.413899	5.16314	0.095289	0.753239	2.26383
253	STF 21b	1	83	2b	Psammite	Monazite	1805.9	Detri.	1800-1825	0.280705	11.5716	11.2035	23.096	0.849255	24.9288	0.073586	0.44851	5.43606	0.274697	2.18798	2.00599
254	STF 21b	1	84	2b	Psammite	Monazite	1855.1	Detri.	1850-1875	0.191622	13.1618	9.44881	21.7348	1.23005	27.8647	0.072483	0.895812	11.277	0.179419	1.09849	1.96254
255	STF 21b	1	85	2b	Psammite	Monazite	1851.4	Detri.	1850-1875	0.379486	13.7449	9.11102	21.8612	1.33255	28.1875	0.069899	0.819992	9.91452	0.264359	1.90451	0.28499
256	STF 21c	1	1	2b	Psammite	Monazite	1744.8	Metam.	1725-1750	0.294311	13.8984	11.1847	22.3285	0.863519	28.2856	0.086139	0.41023	5.23959	0.201218	3.56307	0.206419
257	STF 21c	1	2	2b	Psammite	Monazite	1770.5	Metam.	1750-1775	0.250792	13.7405	11.9225	23.0361	0.789111	28.0309	0.078421	0.399912	4.68743	0.243659	3.31032	0.27029
258	STF 21c	1	3	2b	Psammite	Monazite	1781.8	Metam.	1775-1800	0.202195	14.3626	11.7688	23.2063	0.830048	28.9197	0.071227	0.406206	5.07182	0.223137	3.37064	0.24070
259	STF 21c	1	4	2b	Psammite	Monazite	1759	Metam.	1750-1775	0.25871	14.5872	11.7849	23.6468	0.852945	29.3083	0.07608	0.399431	4.7875	0.251063	3.40864	0.20694
260	STF 21c	1	5	2b	Psammite	Monazite	1771.3	Metam.	1750-1775	0.270481	14.4149	11.5209	22.1959	0.919802	28.9714	0.090344	0.447332	5.28477	0.216162	3.49168	0.23342
261	STF 21c	1	6	2b	Psammite	Monazite	1745.1	Metam.	1725-1750	0.268262	14.2906	11.7627	23.7043	0.833916	28.9239	0.089022	0.364141	4.61789	0.186772	3.18973	0.27584
262	STF 21c	1	7	2b	Psammite	Monazite	1772.2	Metam.	1750-1775	0.245474	14.5228	12.3223	23.5712	0.790284	29.2021	0.071379	0.391597	4.41708	0.202123	3.48139	0.20592
263	STF 21c	1	8	2b	Psammite	Monazite	1749.6	Metam.	1725-1750	0.266172	14.3792	12.0231	23.0709	0.814145	28.8589	0.0763	0.345795	4.24893	0.184154	3.30302	0.29782
264	STF 21c	1	9	2b	Psammite	Monazite	1790.2	Metam.	1775-1800	0.263177	13.9298	11.9921	23.4283	0.93542	28.3926	0.09449	0.307945	4.88208	0.185492	2.94023	1.21467
265	STF 21c	1	10	2b	Psammite	Monazite	1796.4	Metam.	1775-1800	0.250249	14.1158	11.7585	22.2562	0.883803	28.6621	0.064024	0.409073	5.10141	0.170754	3.18442	0.20671
266	STF 21c	1	11	2b	Psammite	Monazite	1756.8	Metam.	1750-1775	0.242342	14.327	11.275	22.6574	0.861789	28.9441	0.080189	0.429161	5.35212	0.261764	3.7355	0.20466
267	STF 21c	1	12	2b	Psammite	Monazite	1770.9	Metam.	1750-1775	0.217534	13.9924	12.2523	23.6907	0.766557	28.3677	0.078568	0.339222	4.17742	0.174464	3.02223	1.21962
268	STF 21c	1	13	2b	Psammite	Monazite	1774	Metam.	1750-1775	0.29596	13.9008	11.8776	23.451	0.884211	28.3868	0.077335	0.399148	4.73975	0.205866	3.03247	0.26662
269	STF 21c	1	14	2b	Psammite	Monazite	1807.2	Detri.	1800-1825	0.280724	13.5076	11.0141	23.0133	1.01552	27.8014	0.082306	0.433082	5.51994	0.226871	3.15768	0.26269
270	STF 21c	1	15	2b	Psammite	Monazite	1771.5	Metam.	1750-1775	0.261971	13.8518	11.7727	23.4119	0.801909	28.2247	0.097397	0.3938	4.77847	0.189614	2.99759	0.28602
271	STF 21c	1	16	2b	Psammite	Monazite	1780.8	Metam.	1775-1800	0.230489	13.6039	12.8039	23.5222	0.835596	27.9725	0.08893	0.371921	4.67504	0.238249	3.33576	0.202157
272	STF 21c	1	17	2b	Psammite	Monazite	1817.8	Detri.	1800-1825	0.191384	13.633	12.5634	23.9854	0.727919	27.8509	0.06371	0.341461	4.29621	0.189594	2.85033	0.20114
273	STF 21c	1	18	2b	Psammite	Monazite	1783.2	Metam.	1775-1800	0.335641	13.5198	11.9153	21.3779	0.999492	27.8561	0.078754	0.462985	5.27887	0.249022	3.37294	1.96152
274	STF 21c	1	19	2b	Psammite	Monazite	1797.9	Metam.	1775-1800	0.217332	14.5482	12.0108	23.2866	0.766079	29.0909	0.078235	0.36074	4.64038	0.20512	3.20117	0.29021
275	STF 21c	1	20	2b	Psammite	Monazite	1765.1	Metam.	1750-1775	0.252804	14.1726	11.4664	22.6719	0.861595	28.7486	0.071867	0.419066	5.35668	0.250689	3.65171	0.20232
276	STF 21c	1	21	2b	Psammite	Monazite	1788	Metam.	1775-1800	0.197413	14.1038	11.9081	22.4784	0.814962	28.6194	0.085289	0.385383	4.9839	0.209718	3.27988	0.24011
277	STF 21c	1	22	2b	Psammite	Monazite	1763.8	Metam.	1750-1775	0.319779	14.1643	11.6325	22.7624	0.892137	28.7432	0.072399	0.410984	5.24216	0.215053	3.36044	0.23815
278	STF 21c	1	23	2b	Psammite	Monazite	1779.5	Metam.	1775-1800	0.254481	14.1121	12.0094	23.0744	0.913968	28.6781	0.078411	0.443585	5.0134	0.239829	3.40983	0.27629
279	STF 21c	1	24	2b	Psammite	Monazite	1758.9	Metam.	1750-1775	0.29762	14.1082	11.6773	23.3586	0.828545	28.5993	0.069191	0.394691	4.9372	0.186373	3.23232	0.24066
280	STF 21c	1	25	2b	Psammite	Monazite	1763.8	Metam.	1750-1775	0.237993	14.3139	11.2021	22.1496	0.813388	28.9449	0.075581	0.401877	5.1255	0.174073	3.74085	1.31927
281	STF 21c	1	26	2b	Psammite	Monazite	1742.4	Metam.	1725-1750	0.569501	13.745	11.5298	22.939	0.953987	28.4033	0.093801	0.381167	4.57268	0.18634	3.28133	1.97229
282	STF 21c	1	27	2b	Psammite	Monazite	1763.7	Metam.	1750-1775	0.293872	13.978	12.0462	22.5691	0.854429	28.419	0.093705	0.357471	4.29782	0.184935	3.02137	0.21819
283	STF 21c	1	28	2b	Psammite	Monazite	1754.7	Metam.	1750-1775	0.327924	13.85	12.3032	24.0691	0.810621	28.342	0.094499	0.32713	4.0888	0.190083	2.85569	1.27777
284	STF 21c	1	29	2b	Psammite	Monazite	1720.9	Metam.	1700-1725	0.225044	13.6464	11.9455	23.4345	0.836167	27.9366	0.076536	0.379711	4.61376	0.218706	3.06853	0.25607
285	STF 21c	1	30	2b	Psammite	Monazite	1795.6	Metam.	1775-1800	0.220241	13.6533	11.5301	22.7892	0.864306	27.9994	0.074505	0.439411	5.32735	0.266802	3.40798	0.25006
286	STF 21c	1	31	2b	Psammite	Monazite	1774.7	Metam.	1750-1775	0.231846	14.4404	11.5725	23.2657	0.764383	29.0469	0.077243	0.384859	4.92238	0.224523	3.46127	1.23642
287	STF 21c	1	32	2b	Psammite	Monazite	1778.4	Metam.	1775-1800	0.4959	14.3759	12.016	23.5785	0.825497	29.2192	0.078006	0.356648	4.55152	0.149962	3.03964	1.20753
288	STF 21c	1	33	2b	Psammite	Monazite	1780.9	Metam.	1775-1800	0.272901	14.3371	11.0179	23.1834	0.891269	28.9592	0.064509	0.393317	5.19907	0.186016	3.30654	0.26565
289	STF 21c	1	34	2b	Psammite	Monazite	1721.1	Metam.	1700-1725	0.253443	14.0539	11.8315	23.227	0.809858	28.511	0.080503	0.363112	4.6172	0.244114	3.34706	0.25446
290	STF 21c	1	35	2b	Psammite	Monazite	1752	Metam.	1750-1775	0.357728	14.108	11.8118	23.1689	0.919633	28.7164	0.086835	0.361275	4.46789	0.174375	3.32838	0.25943
291	STF 21c	1	36	2b	Psammite	Monazite	1754.9	Metam.	1750-1775	0.255445	14.2822	11.2053	22.7129	0.844835	28.9108	0.046591	0.426973	5.31358	0.226631	3.848	0.21889
292	STF 21c	1	37	2b	Psammite	Monazite	1777.3	Metam.	1775-1800	0.236077	14.0625	12.6907	24.249	0.780224	28.5151	0.071022	0.315468	3.99007	0.218385	2.85431	0.261
293	STF 21c	1	38	2b	Psammite	Monazite	1782.7	Metam.	1775-1800	0.191613	14.2471	11.9466	23.5697	0.746745	28.7473	0.097085	0.342522	4.45731	0.216515	3.41285	0.24027
294	STF 21c	1	39	2b	Psammite	Monazite	1773.7	Metam.	1750-1775	0.37506	14.0404	11.3786	22.8879	1.15327	28.6228	0.098256	0.534623	5.68355	0.43624	2.56438	2.1029
295	STF 21c	1	40	2b	Psammite	Monazite	1749.5	Metam.	1725-1750	0.30906	14.0106	12.4196	22.9223	0.860342	28.51	0.08411	0.342056	4.44444	0.162041	2.69983	0.25479
296	STF 21c	1	41	2b	Psammite	Monazite	1767	Metam.	1750-1775	0.206048	14.2539										

364	STF 21c	2	49	2b	Psammite	Monazite	1756.8	Metam.	1750-1775	0	0.27917	14.2358	11.1267	22.2192	0.967985	28.8684	0.071251	0.504226	5.74409	0.278978	3.92043	1.98516
365	STF 21c	2	50	2b	Psammite	Apatite	4159.4	Unkn.		0	0.051567	19.5429	0.083452	0.109066	37.6662	40.4743	0.116224	0.006253	0	0	0.218754	0
366	STF 22	1	1		Granit Igneous	Monazite	1801.6	Igneous		0	0.142087	13.9793	10.8871	22.908	1.14224	27.994	0.062695	0.688276	6.1908	0.758308	2.05849	1.92666
367	STF 22	1	2		Granit Igneous	Monazite	1763.7	Igneous		0	0.283248	13.8488	9.87688	22.3518	1.06138	28.0404	0.067444	0.659266	7.31451	0.396714	2.17113	2.11712
368	STF 22	1	3		Granit Igneous	Monazite	1753.3	Igneous		0	0.271013	13.8536	10.2707	22.6502	1.07055	28.0946	0.078355	0.635888	7.08469	0.434014	2.25306	2.00594
369	STF 22	1	4		Granit Igneous	Monazite	1784.3	Igneous		0	0.287309	13.6836	9.67793	21.9722	1.0811	27.9313	0.078392	0.647728	7.53338	0.323188	2.86011	2.09623
370	STF 22	1	5		Granit Igneous	Monazite	1790	Igneous		0	0.224961	14.0376	9.9425	22.4692	1.02152	28.3254	0.074855	0.561161	6.88094	0.278728	2.74219	2.01092
371	STF 22	1	6		Granit Igneous	Monazite	1779.6	Igneous		0	0.274112	13.6761	9.71844	20.891	1.1179	27.3343	0.068163	0.804232	5.64328	0.812071	2.78612	1.96028
372	STF 22	1	7		Granit Igneous	Monazite	1805.4	Igneous		0	0.302137	13.8967	9.52196	21.8476	1.15397	28.2284	0.07567	0.74015	7.72356	0.450206	2.7678	2.01716
373	STF 22	1	8		Granit Igneous	Monazite	1765.3	Igneous		0	0.295567	13.9782	9.48639	21.8277	1.09335	28.3082	0.075975	0.644616	7.42971	0.377144	2.99088	1.94598
374	STF 22	1	9		Granit Igneous	Monazite	1775.2	Igneous		0	0.279497	13.9343	9.58998	21.8041	1.00152	28.1753	0.06898	0.563345	6.86107	0.343066	3.3326	1.93045
375	STF 22	1	10		Granit Igneous	Monazite	1810	Igneous		0	0.271273	13.9153	9.85339	22.3763	1.0697	28.1665	0.060849	0.654255	7.23042	0.396901	2.40526	2.07063
376	STF 22	1	11		Granit Igneous	Monazite	1770.5	Igneous		0	0.330434	13.798	9.26758	21.6525	1.10545	28.0689	0.062773	0.694066	7.92171	0.331156	2.88984	2.07299
377	STF 22	1	12		Granit Igneous	Monazite	1780.3	Igneous		0	0.305165	13.8999	9.88136	22.6779	1.02903	28.1035	0.082534	0.609018	6.97846	0.366146	2.50272	2.03233
378	STF 22	1	13		Granit Igneous	Monazite	1781.6	Igneous		0	0.267959	13.8616	9.69592	22.278	1.32947	28.1199	0.080907	0.942466	7.3345	1.30936	2.88373	1.88772
379	STF 22	1	14		Granit Igneous	Monazite	1783.9	Igneous		0	0.148238	13.7602	10.317	20.6665	0.938513	27.1297	0.07917	0.48379	5.32516	0.31808	2.92722	1.88987
380	STF 22	1	15		Granit Igneous	Monazite	1804	Igneous		0	0.21598	13.584	10.0358	21.5453	1.0992	27.0606	0.085981	0.640717	6.84649	0.462985	1.22782	2.00999
381	STF 22	1	16		Granit Igneous	Monazite	1780.5	Igneous		0	0.174951	13.9787	11.053	22.632	0.990866	27.9358	0.077866	0.474821	5.7958	0.296519	2.1909	1.9439
382	STF 22	1	17		Granit Igneous	Monazite	1763.3	Igneous		0	0.275336	13.8416	9.43145	21.2625	1.00249	28.0758	0.058696	0.579206	6.89894	0.33593	3.52877	2.01894
383	STF 22	1	18		Granit Igneous	Monazite	1788.2	Igneous		0	0.277549	13.519	9.47512	21.0056	1.02799	27.1234	0.080384	0.6212	6.93343	0.415194	2.20011	1.9547
384	STF 22	1	19		Granit Igneous	Monazite	1790.1	Igneous		0	0.233852	13.8327	9.48634	21.197	1.09332	27.7962	0.065059	0.710571	6.69349	0.600281	3.01384	1.9827
385	STF 22	1	20		Granit Igneous	Monazite	1784.8	Igneous		0	0.243036	13.7744	9.70969	21.137	1.03827	27.46	0.070712	0.67104	6.76024	0.607685	2.03125	2.01654
386	STF 22	1	21		Granit Igneous	Monazite	1762.6	Igneous		0	0.248639	13.6021	9.26553	20.8344	0.90989	27.2269	0.058168	0.520134	6.17495	0.296971	3.2892	1.86366
387	STF 22	1	22		Granit Igneous	Monazite	1773.5	Igneous		0	0.247374	14.2514	11.2051	23.8738	0.9347	28.7445	0.091151	0.530195	5.73573	0.29764	2.46896	2.03867
388	STF 22	1	23		Granit Igneous	Monazite	1785.8	Igneous		0	0.302633	13.7382	9.76755	22.2305	1.06383	27.8713	0.076512	0.622703	7.20476	0.347955	2.2014	2.05064
389	STF 22	1	24		Granit Igneous	Monazite	1775.1	Igneous		0	0.259005	13.9203	10.5833	22.0766	1.12279	28.1159	0.07752	0.664938	7.13088	0.550928	1.41698	2.02538
391	STF 22	1	26		Granit Igneous	Monazite	1776.6	Igneous		0	0.264239	13.3845	9.49313	20.9233	1.03508	26.8984	0.062134	0.621671	1.60634	0.294395	2.21368	1.82842
392	STF 22	1	27		Granit Igneous	Monazite	1757.2	Igneous		0	0.263929	13.253	9.95859	19.7327	0.943	26.4851	0.068038	0.566746	7.10837	0.333695	2.74273	1.80741
393	STF 22	1	28		Granit Igneous	Monazite	1784.7	Igneous		0	0.237628	13.1385	8.6509	19.7344	0.92967	26.1322	0.063878	0.519659	6.66048	0.28817	2.75404	1.84201
394	STF 22	1	29		Granit Igneous	Monazite	1760.9	Igneous		0	0.236561	13.9731	9.86076	20.7066	1.1296	28.1553	0.074445	0.685388	7.08055	0.549657	2.45571	2.01059
395	STF 22	1	30		Granit Igneous	Monazite	1784	Igneous		0	0.276267	13.3086	8.95503	20.2506	0.958825	26.6245	0.063379	0.605246	6.84865	0.340859	2.78436	1.86396
396	STF 22	1	31		Granit Igneous	Monazite	1770.6	Igneous		0	0.318783	13.8052	9.15163	21.4196	1.11751	28.0127	0.06623	0.653336	7.7276	0.360855	3.00159	2.06576
397	STF 22	1	32		Granit Igneous	Monazite	1763.2	Igneous		0	0.280839	14.0682	9.58522	22.0999	1.05781	28.4714	0.068767	0.585748	7.30294	0.325139	2.97832	2.11166
398	STF 22	1	33		Granit Igneous	Monazite	1757.2	Igneous		0	0.270516	13.7599	9.39649	21.8116	1.03296	27.9222	0.074819	0.602013	7.18095	0.311835	2.9272	2.08688
399	STF 22	1	34		Granit Igneous	Monazite	1740.2	Igneous		0	0.232697	13.9678	10.1742	22.3894	0.872444	28.1695	0.065537	0.534265	5.74103	0.346522	3.23221	2.02714
400	STF 22	1	35		Granit Igneous	Monazite	1746.2	Igneous		0	0.184032	13.9088	10.8123	22.5473	1.07679	28.8898	0.089141	0.654307	5.94886	0.667717	2.09891	1.96387
401	STF 22	1	36		Granit Igneous	Monazite	1759.8	Igneous		0	0.266497	13.899	10.2131	22.8338	1.07656	28.1657	0.092784	0.638363	7.2344	0.428244	2.03188	2.06364
402	STF 22	1	37		Granit Igneous	Monazite	1795.1	Igneous		0	0.282763	13.906	9.73152	22.7076	1.0543	28.0586	0.07283	0.632543	7.2038	0.42108	2.26852	2.06241
403	STF 22	1	38		Granit Igneous	Monazite	1764.2	Igneous		0	0.277994	13.8366	10.0222	22.6451	1.07136	28.0363	0.087114	0.665236	7.16151	0.422425	2.0203	2.05041
404	STF 22	1	39		Granit Igneous	Monazite	1772.6	Igneous		0	0.280762	13.8813	9.68043	22.2465	1.03857	28.1806	0.083975	0.670195	7.10531	0.40954	2.66812	2.12127
405	STF 22	1	40		Granit Igneous	Monazite	1779.5	Igneous		0	0.294587	13.9869	8.60045	21.7746	1.23374	28.331	0.072781	0.807994	7.80102	0.714273	2.82725	1.93294
406	STF 22	1	41		Granit Igneous	Monazite	1755.2	Igneous		0	0.303457	13.7967	9.52292	22.0261	1.18042	28.0334	0.071871	0.733141	7.77264	0.527058	2.56587	1.99639
407	STF 22	1	42		Granit Igneous	Monazite	1815.7	Igneous		0	0.180412	13.6581	9.30507	20.5267	1.09403	27.2277	0.07768	0.59408	6.82753	0.335145	2.89239	1.79886
408	STF 22	1	43		Granit Igneous	Monazite	1781.9	Igneous		0	0.28026	13.8143	9.94284	22.4687	1.05426	27.9734	0.069502	0.636747	7.36971	0.402334	2.1141	2.07064
409	STF 22	1	44		Granit Igneous	Monazite	1772.2	Igneous		0	0.152306	14.1319	10.7915	22.8344	1.07685	28.2837	0.07275	0.611478	5.9601	0.584883	2.28148	2.05377
410	STF 22	1	45		Granit Igneous	Monazite	1763.8	Igneous		0	0.305202	13.8389	9.40612	21.5314	1.07602	28.0785	0.076538	0.656507	7.49632	0.332411	3.10492	2.05589
411	STF 22	1	46		Granit Igneous	Monazite	1758.3	Igneous		0	0.167027	14.0933	10.4904	22.5444	1.05523	28.1561	0.065947	0.638152	5.97338	0.880435	2.50572	1.96561
412	STF 22	1	47		Granit Igneous	Monazite	1753.6	Igneous		0	0.291173	13.1076	9.39247	22.4284	0.990035	26.9653	0.076657	0.597766	6.88027	0.332143	3.22199	1.9549
413	STF 22	1	48		Granit Igneous	Monazite	1762.4	Igneous		0	0.300951	13.7787	9.46357	22.0752	1.071098	0.639387	0.741619	0.359965	6.30176	0.20186	2.44043	2.00685
414	STF 22	1	49		Granit Igneous	Monazite	1764.6	Igneous		0	0.291236	13.932	9.67963	21.9401	1.03408	28.2318	0.073252	0.644444	7.11995	0.397329	3.07663	1.97359
415	STF 22	1	50		Granit Igneous	Monazite	1749.3	Igneous		0	0.273968	13.8765	9.83432	22.3478	1.091842	28.0698	0.099162	0.522906	6.4067	0.274835	3.00502	2.02685
416	STF 22	1	51		Granit Igneous	Monazite	0	Igneous		0	0.233906	14.0663	9.88167	22.1487	1.16047	28.2905	0.084596	0.597483	7.50524	0.28038	3.21519	1.95336
417	STF 22	1	52		Granit Igneous	Monazite	0	Igneous		0	0.310904	13.8064	9.51297	22.0674	1.07865	28.0438	0.063648	0.615503	7.39729	0.306182	2.78696	2.1179

APPENDIX C: MONAZITE GEOCHRONOLOGICAL DATA

Table with columns: Sample, Run #, Grain ID, Pb207/Pb206, 1s, Pb207/206, 1s, Err Correction, Err% 7-6, Err% 6-238, Err% 7-235, Pb207/Pb206, 1s, Pb207/206, 1s, Pb207/206, 1s, Pb204, Pb206, Pb207, U238. This is a large data table containing multiple columns of numerical values representing isotopic ratios and errors.

STF 21b 1	MN247	0.1112	0.00139	4.80581	0.08885	0.31362	0.00546	0.795984017	1.125	1.7409604	1.848804	1819.1	22.54	24.68	1785.9	15.54	0	417265	46869	2238902		
STF 21b 1	MN248	0.11629	0.00133	5.2617	0.09318	0.32839	0.00568	0.786760371	1.143692	1.7295607	1.770911	1899.9	20.49	18.77	1830.6	27.56	1862.7	15.11	10	492247	58549	2574732
STF 21b 1	MN249	0.11037	0.00215	4.67236	0.08262	0.30722	0.00534	0.791483539	1.132554	1.7381681	1.768271	1805.5	20.39	17.27	1662.3	17.62	1763.3	14.79	9	201208	22697	1129964
STF 21b 1	MN250	0.11533	0.00144	5.10226	0.09415	0.32104	0.00559	0.797904968	1.248591	1.741216	1.845261	1885.1	22.39	19.94	1872.8	27.28	1836.5	15.67	6	190458	22246	1020730
STF 21b 1	MN251	0.11345	0.00153	4.91583	0.10045	0.34783	0.00529	0.793471657	1.227827	1.7537358	1.837488	1850.3	22.79	19.21	188.1	29.13	1887.4	15.9	27	91213	10515	453676
STF 21b 1	MN252	0.1115	0.00124	4.90463	0.08632	0.31919	0.00527	0.797997368	1.112058	1.7387763	1.75997	1824	20.06	17.85	17.11	1803.1	14.84	8.01	5	501879	57367	2718479
STF 21b 1	MN253	0.11413	0.00135	5.05031	0.0905	0.32108	0.00556	0.775138439	1.182862	1.7316557	1.791969	1866.1	21.13	17.95	17.13	1827.8	15.19	27	591272	69009	3168161	
STF 21b 1	MN254	0.11479	0.00136	5.15749	0.09246	0.326	0.00565	0.774683595	1.184772	1.7331288	1.792733	1876.1	21.17	1819	27.46	1845.6	15.25	20	444100	52131	2340607	
STF 21b 1	MN255	0.11504	0.00175	5.31053	0.10703	0.33526	0.00598	0.686513615	1.52121	1.7836903	1.201543	1880.4	27.16	1863.8	28.87	1870.6	17.22	0	59871	7065	3088146	
STF 21b 1	MN256	0.10788	0.00113	5.05453	0.08532	0.3398	0.00508	0.806966047	1.04746	1.7068864	1.687991	1763.9	19.04	1885.7	28.89	1828.5	14.31	12	2147148	240012	10741908	
STF 21b 1	MN257	0.1086	0.00118	4.75414	0.08115	0.31747	0.00542	0.797436506	1.086556	1.7027429	1.706933	1876.2	19.08	1777.4	26.5	1776.8	14.32	0	150733	17612	835880	
STF 21b 1	MN258	0.11102	0.0013	5.17178	0.0893	0.33195	0.00568	0.764127395	1.17096	1.680722	1.726678	1812.6	21.09	19.87	27.36	1848	14.69	19	108651	12386	533847	
STF 21b 1	MN259	0.11161	0.00128	5.1609	0.08601	0.32484	0.0055	0.810594989	1.035599	1.693144	1.71386	1878.5	18.54	1813.3	26.75	1843.1	14.21	7	321302	38071	1686662	
STF 21b 1	MN260	0.11199	0.00116	5.13981	0.09537	0.33264	0.00523	0.80446746	1.172529	1.662104	1.674589	1830.3	18.68	1851.2	26.56	1801.2	15.13	28	300045	38196	1679146	
STF 21b 1	MN261	0.11384	0.00128	5.25326	0.09308	0.33469	0.00571	0.78414505	1.124885	1.7005654	1.7075	1861.7	21.03	1861.1	27.56	1861.2	14.68	7	50466	5917	2568476	
STF 21b 1	MN262	0.11253	0.00117	5.10075	0.08582	0.32883	0.00558	0.810720223	1.039723	1.6969255	1.682498	1840.7	18.75	1832.7	27.08	1836.2	14.28	16	792714	91826	4079751	
STF 21b 1	MN263	0.11016	0.00122	5.05122	0.08646	0.33272	0.00565	0.789045695	1.10748	1.6981245	1.711666	1840.2	19.95	1851.5	27.34	1828	14.51	0	184360	20910	931523	
STF 21b 1	MN264	0.11307	0.00123	5.13128	0.09055	0.35369	0.00608	0.800374955	1.087822	1.7190195	1.724619	1849.4	19.55	1952.2	28.96	1902.6	14.82	16	369874	43093	1788877	
STF 21b 1	MN265	0.11104	0.00123	5.06202	0.08577	0.33068	0.00564	0.808797406	1.053674	1.7055764	1.674188	1816.5	18.99	1841.7	27.31	1829.6	14.37	17	409422	46776	2013186	
STF 21b 1	MN266	0.1093	0.00121	5.17135	0.08983	0.34322	0.00591	0.795173194	1.107405	1.7219276	1.730791	1787.8	20.07	1902.2	28.35	1847.9	14.78	4	232994	26191	1161196	
STF 21b 1	MN267	0.10791	0.00116	4.84309	0.08267	0.32566	0.00555	0.801381946	1.074097	1.7042314	1.706987	1764.5	19.49	1817.3	27	1792.4	14.37	0	218842	24290	1144031	
STF 21b 1	MN268	0.11461	0.00125	5.28447	0.09187	0.33878	0.00585	0.795104589	1.11390	1.7267843	1.746604	1838.8	20	1880	28.16	1896.5	14.9	14	224018	25849	1131348	
STF 21b 1	MN269	0.11414	0.00126	5.16129	0.0975	0.35527	0.00613	0.797873706	1.099295	1.7198187	1.73104	1874.2	19.76	1959.7	29.07	1918.1	14.97	3	149498	23298	938507	
STF 21b 1	MN270	0.11086	0.00129	5.62472	0.09291	0.3449	0.00591	0.776919152	1.16363	1.7193389	1.727102	1813.6	21.04	1910.2	28.41	1863.9	15.05	3	108181	12334	533576	
STF 21b 1	MN271	0.11091	0.00114	5.00119	0.08438	0.32721	0.00559	0.816890945	1.02786	1.708383	1.687198	1814.3	18.55	1824.8	27.13	1819.5	14.28	14	370892	42211	1930382	
STF 21b 1	MN272	0.1082	0.00121	4.73608	0.08327	0.31763	0.00551	0.79507459	1.118299	1.7347228	1.758205	1769.2	20.27	1782.2	26.95	1773.6	14.74	11	279478	30923	1516289	
STF 21b 1	MN273	0.11081	0.00116	4.70401	0.07939	0.30804	0.00523	0.808796726	1.046837	1.6978315	1.687709	1812.7	18.94	1731.1	25.5	1768	14.13	7	305916	34843	1681925	
STF 21b 1	MN274	0.11313	0.00125	5.10677	0.08714	0.32763	0.00555	0.788764763	1.104924	1.6939841	1.705728	1850.3	19.87	1826.9	26.93	1837.5	14.48	0	106089	12347	544243	
STF 21b 1	MN275	0.11302	0.00127	5.11609	0.08951	0.32845	0.00566	0.790710359	1.123695	1.7232455	1.749578	1848.6	21.08	1830.9	27.46	1838.8	14.86	0	89421	10325	465460	
STF 21b 1	MN276	0.11248	0.00121	4.95224	0.08496	0.31947	0.00546	0.80266739	1.075747	1.7098007	1.715587	1839.9	19.38	1781.7	26.68	1811.2	14.69	6	466144	53697	2483543	
STF 21b 1	MN277	0.11562	0.00123	5.04361	0.08825	0.3315	0.00544	0.795007862	1.124321	1.7215255	1.737499	1871.8	20.56	1785.6	26.02	1781.7	14.26	26	256499	60545	273016	
STF 21b 1	MN278	0.11023	0.00133	4.78181	0.08117	0.31915	0.00532	0.773908315	1.131555	1.6669278	1.694734	1777.8	20.56	1785.6	26.02	1781.7	14.26	26	304167	34061	1578020	
STF 21b 1	MN279	0.11651	0.00142	4.59346	0.09006	0.33999	0.00588	0.761527833	1.21878	1.7294626	1.796181	1903.4	21.7	1886.6	28.28	1894.2	15.41	0	61713	7363	30654	
STF 21b 1	MN280	0.11342	0.00121	5.01304	0.08474	0.32071	0.00542	0.808008921	1.066831	1.6900003	1.690391	1855	19.88	1793.2	26.44	1821.5	14.31	0	548370	63798	2877332	
STF 21b 1	MN281	0.11117	0.00121	4.72688	0.08141	0.31153	0.00528	0.795132732	1.088423	1.6948608	1.70575	1818.6	19.64	1748.3	25.96	1780.1	14.32	13	357531	40793	1936483	
STF 21b 1	MN282	0.11295	0.00142	4.74715	0.10082	0.35169	0.00615	0.755969792	1.257193	1.7489991	1.841747	1847.4	22.57	1942.4	29.31	1896.5	15.81	6	94455	10886	462720	
STF 21b 1	MN283	0.1104	0.00139	4.66996	0.0836	0.30689	0.00518	0.739416607	1.259058	1.6876912	1.790165	1805.9	22.7	1925.6	25.56	1761.9	14.97	0	350202	40431	1944538	
STF 21b 1	MN284	0.11332	0.00137	4.92923	0.08909	0.31536	0.00544	0.787149323	1.207793	1.7250127	1.803782	1851.1	21.71	1767	26.65	1807.3	15.26	7	250041	29343	1381063	
STF 21b 1	MN285	0.11342	0.00128	5.11099	0.08767	0.32764	0.00552	0.778943207	1.130742	1.684776	1.710833	1854.1	20.32	1826.9	26.81	1837.9	15.27	18	117900	13693	601840	
STF 21c 1	MN201	0.10796	0.00115	4.85175	0.07676	0.32958	0.00516	0.764914559	1.077832	1.565620	1.576132	1748.8	18.61	1836.4	25.02	1790.8	13.27	10	139470	1900	638090	
STF 21c 1	MN202	0.10827	0.00121	4.73165	0.07444	0.31463	0.00495	0.763388884	1.071825	1.565184	1.576568	1771.5	19.57	1710.5	24.24	1771.1	13.27	10	159161	17815	784617	
STF 21c 1	MN203	0.10895	0.00118	4.77433	0.0756	0.31783	0.00498	0.763636187	1.083066	1.5668754	1.583468	1781.8	19.72	1791.4	24.34	1780.4	13.27	16	151313	17228	751147	
STF 21c 1	MN204	0.10759	0.00117	4.77009	0.07561	0.32156	0.00503	0.761614511	1.087462	1.5642493	1.585085	1759.9	19.7	1797.3	24.54	1779.6	13.31	8	191183	21217	926772	
STF 21c 1	MN205	0.10832	0.00119	4.72981	0.07541	0.3167	0.00496	0.758486696	1.098597	1.5661509	1.594356	1771.3	20	1737.6	24.27	1772.3	13.36	26	170287	19287	850422	
STF 21c 1	MN206	0.10678	0.00119	4.70642	0.07556	0.31969	0.00501	0.753475391	1.114441	1.5671432	1.605467	1745.1	20.32	1788.2	24.45	1768.4	13.45	23	153521	16873	748365	
STF 21c 1	MN207	0.10837	0.00122	4.75839	0.07666	0.31847	0.00499	0.74935371	1.125773	1.5668666	1.611049	1772.2	20.42	1782.2	24.38	1777.6	13.52	20	168406	18764	823950	
STF 21c 1	MN208	0.10704	0.00121	4.70035	0.07602	0.31851	0.00499	0.748349799	1.130419	1.5666698	1.617326	1790.2	20.51	1782.5	24.38	1767.3	13.54	0	190203	20909	930346	
STF 21c 1	MN209	0.10945	0.00126	4.72513	0.07701	0.31315	0.00491	0.747843957	1.151211	1.5679387	1.629796	1792.6	20.83	1785.2	24.08	1771.7	13.66	29	162148	18207	806604	
STF 21c 1	MN210	0.10746	0.00128	4.73785	0.07895	0.314																

Table with columns for ID, Name, and various numerical values. The table contains approximately 100 rows of data, with some cells containing text like '###' or '###' indicating missing or specific data points.